

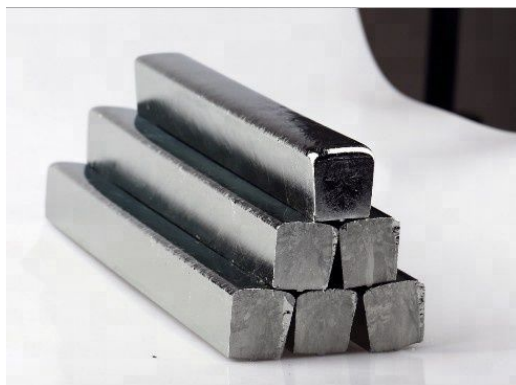
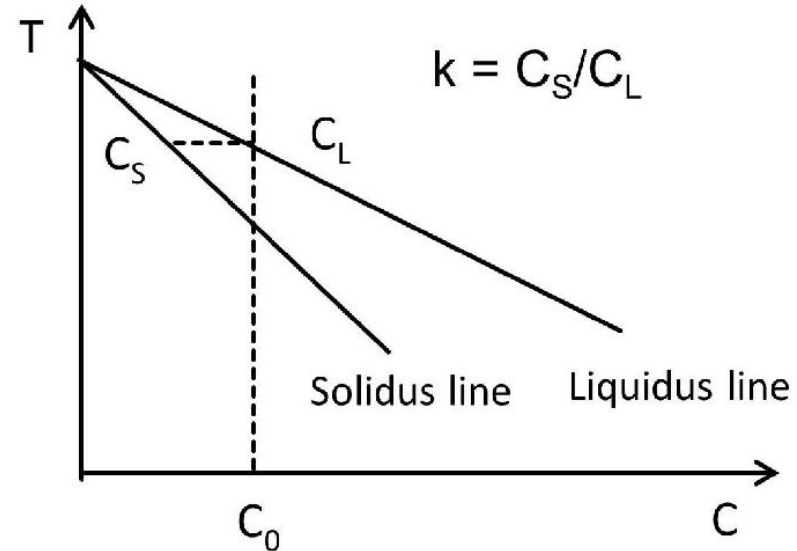
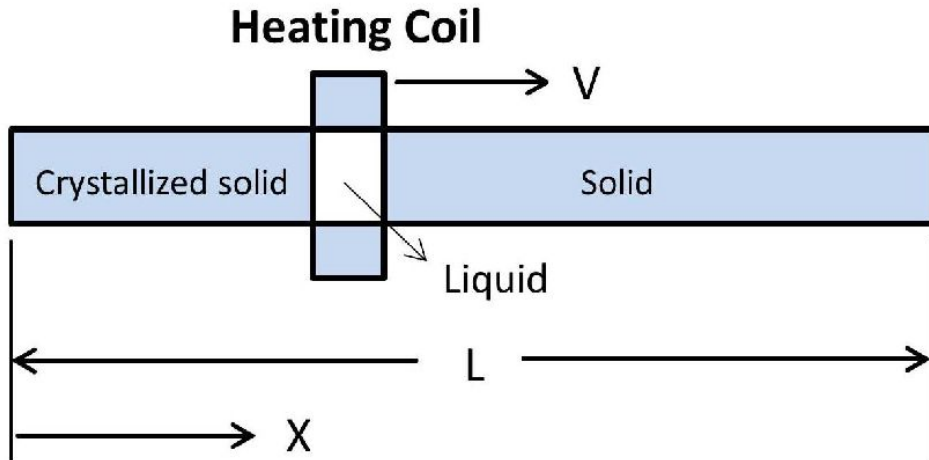
Germanium detectors and their application in science

Marco Salathe

Lawrence Berkeley National Laboratory

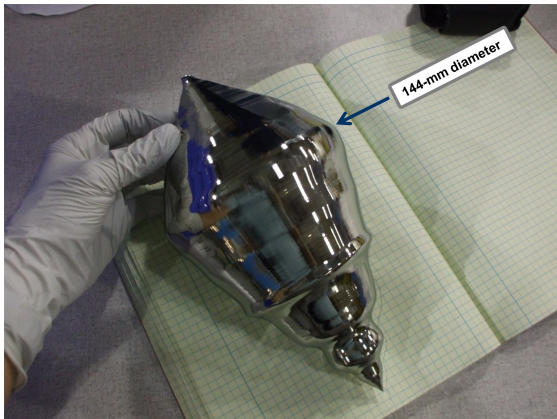
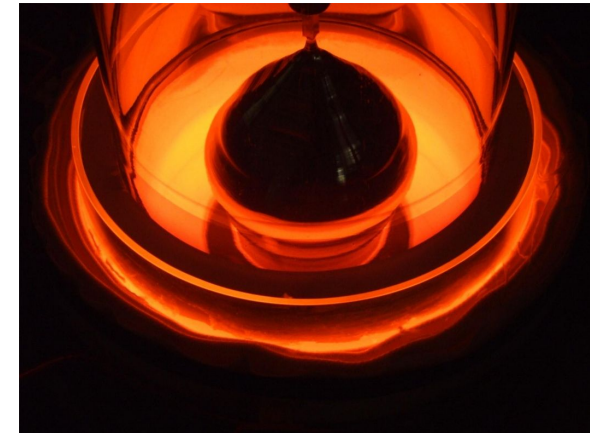
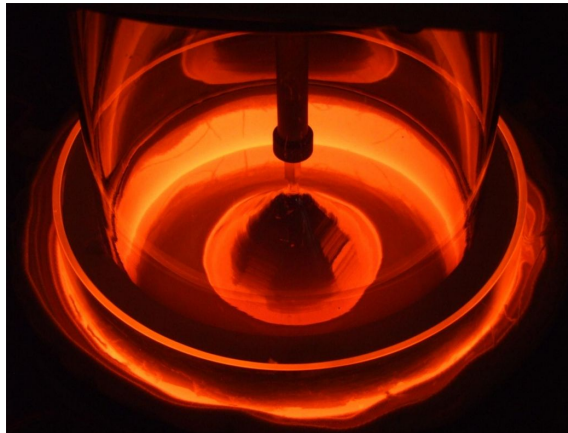
NE204, Sept. 13, 2018

Germanium zone refining



- W. L. Hansen and E. E. Haller, IEEE Transactions on Nuclear Science, vol. 21, no. 1, pp. 251-259, Feb. 1974. doi: 10.1109/TNS.1974.4327469
- Xiaoxin Zhang, Semiramis Friedrich, Bernd Friedrich, Journal of Crystallization Process and Technology, Vol.8 No.1, 2018. 10.4236/jcpt.2018.81003
- https://www.alibaba.com/product-detail/Top-one-99-9999-germanium-metal_60680199404.html
- Final material is either n-type or p-type (depending on remaining impurities), certain material are preferred in certain application
 - Less trapping in p-type
 - Less neutron damage in n-type

Germanium chrystral pulling

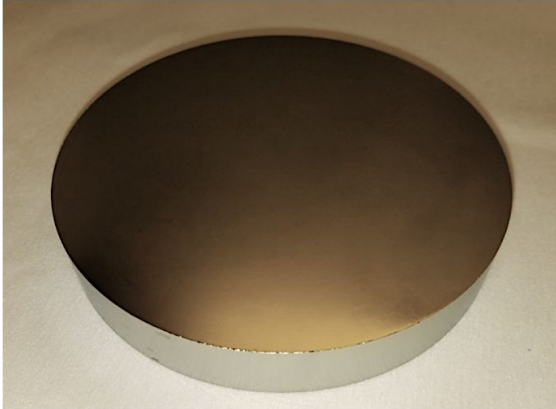


Detector production

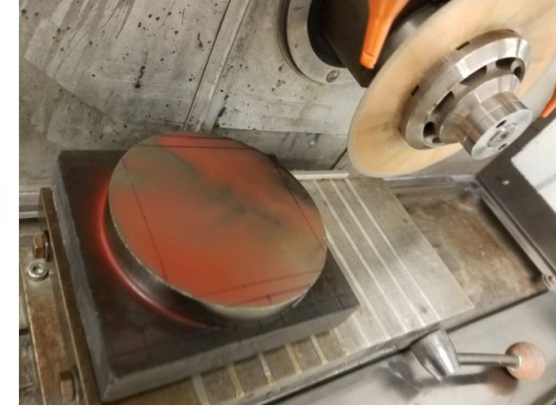
As received



Pre-etched



During cutting



After cutting



During Lapping

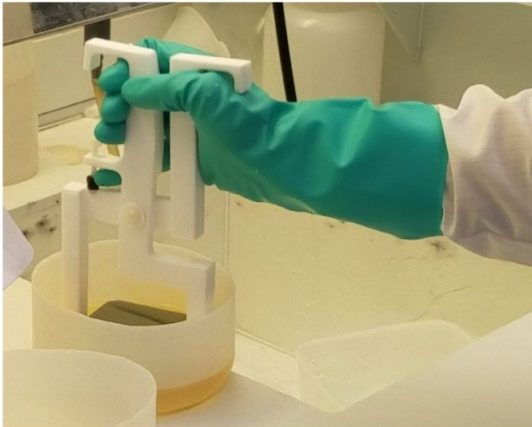


After lapping

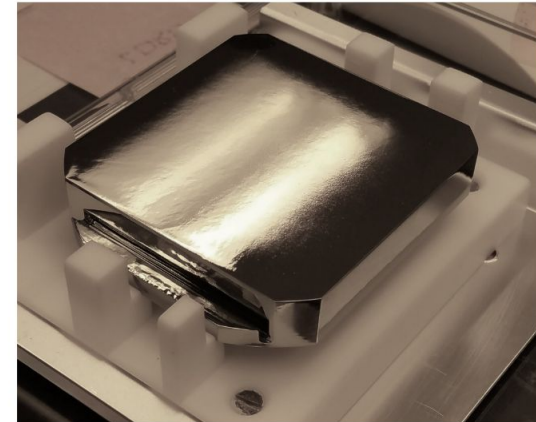


Detector production

During Etching

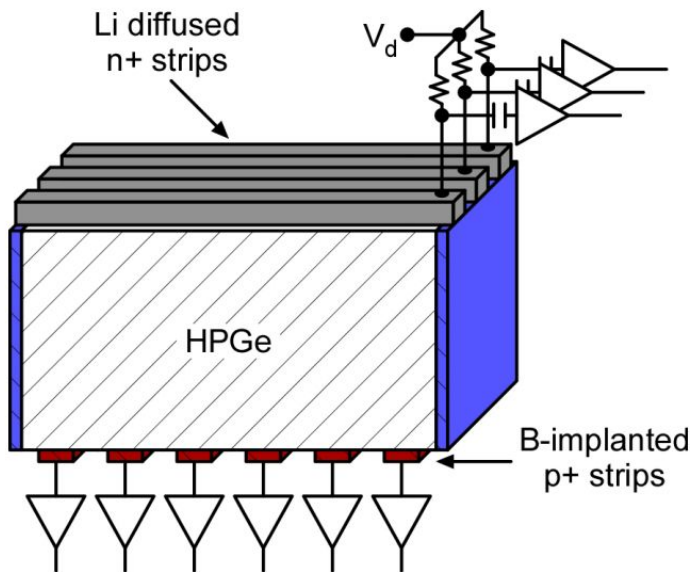


After Etching



- Sputter or diffuse electronic contacts on surface
 - Lithium diffusion (forming n-type contact)
 - Boron implantation (forming p-type contact)
 - Amorphous germanium plus metal layer (can form either contact)
- Passivate exposed surfaces

Classical diode layout



Li-diffused contact:

- Thick (large dead layer and difficult to finely segment)
- Li readily diffuses at room temperature
- Limited to coarse segmentation (~1 mm pitch), D. Gutknecht, NIM A288, 13 (1990)
- Requires additional processing to passivate surfaces between contact segments

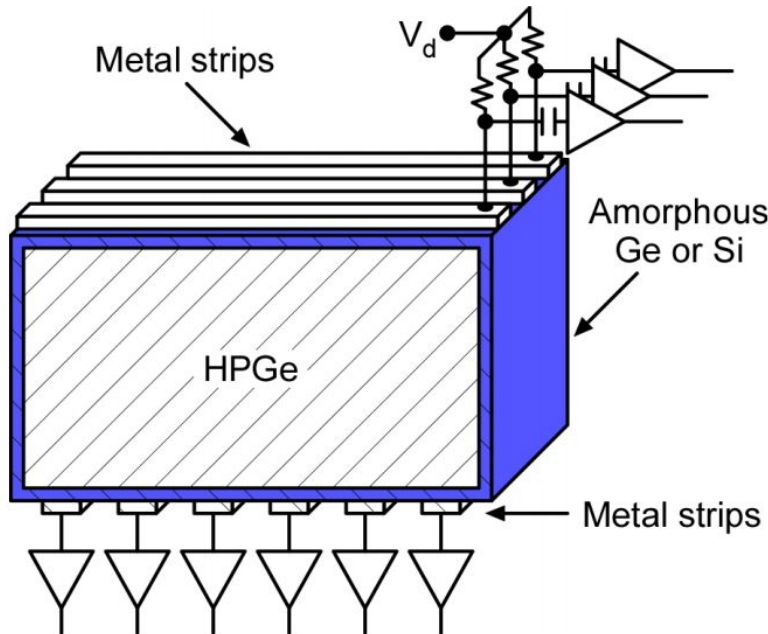
B-implanted contact:

- Requires additional processing to passivate surfaces between contact segments
- S.R. Amendolia, ..., E.E. Haller et al.,
NIM 226, 117 (1984)

Is inter-contact surface passivation necessary?

Unpassivated inter-contact strip detectors: D. Protic and G. Riepe, IEEE TNS 32, 553 (1985); D. Protic and T. Krings, IEEE TNS 50, 998 (2003)

Amorphous contact layout



Advantages:

- Simple fabrication
- Thin contact dead layer
- Complete surface passivation: a-Ge is commonly used for surface passivation on Ge detectors
- Fine achievable contact pitches
- Bipolar blocking

Issues:

- Not as rugged as diffused or implanted contacts
- Not as effective at blocking carrier injection as are impurity contacts
- Other potential ones to be discussed

W.L. Hansen and E.E. Haller, IEEE TNS 24, 61 (1977) → A-Ge electrical contact on HPGe

W.L. Hansen, E.E. Haller, G.S. Hubbard, IEEE TNS 27, 247 (1980) → A-Ge passivation on HPGe

P.N. Luke, et al., IEEE TNS 39, 590 (1992) → Demonstrated bipolar blocking, thin dead layer, segmentation

Shockley Ramo Theorem

Quasi steady-state approximation (the field configuration at a given moment in time is static):

- The trajectory of charge carrier is defined by the interaction position, the electric field \vec{E} and the mobility μ_e : $\vec{v}_e = \mu_e \vec{E}$.
- At each position along the trajectory Gauss' Law defines the induced charge Q_i into an electrode by a charge carrier of charge q :

$$Q_i = \iint_S \varepsilon \vec{E} \cdot d\vec{S}, \quad (1)$$

Shockley-Ramo theorem¹:

- Calculate the induced charge Q_i on an electrode from the weighting potential $\psi_i(\vec{x})$ defined as follow:

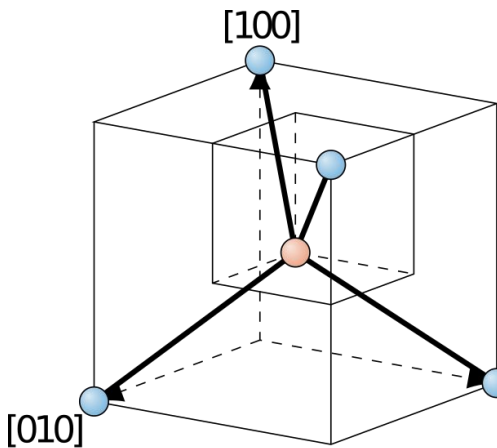
$$\nabla^2 \psi_i(\vec{x}) = 0, \quad \psi_i(\vec{x})|_{S_j} = \delta_{ij} \quad (2)$$

- The induced charge Q_i is then:

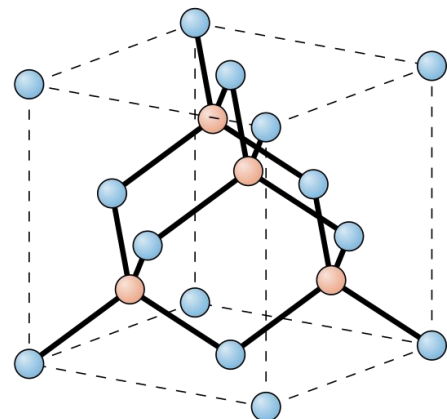
$$q\psi_i(\vec{x}) = Q_i. \quad (3)$$

- The change in the induced charge Q_i correspond to the observed current in the read out circuit

Crystal structure

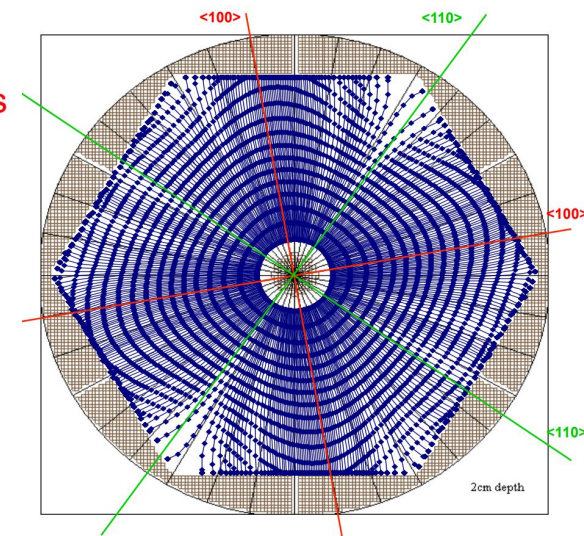
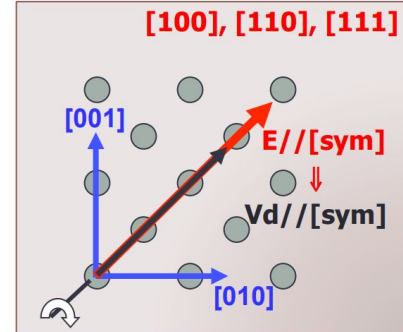
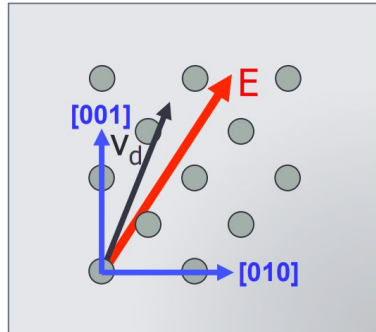
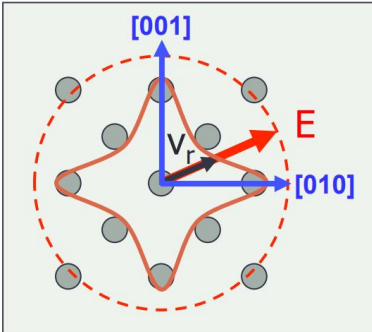


Radial anisotropy,

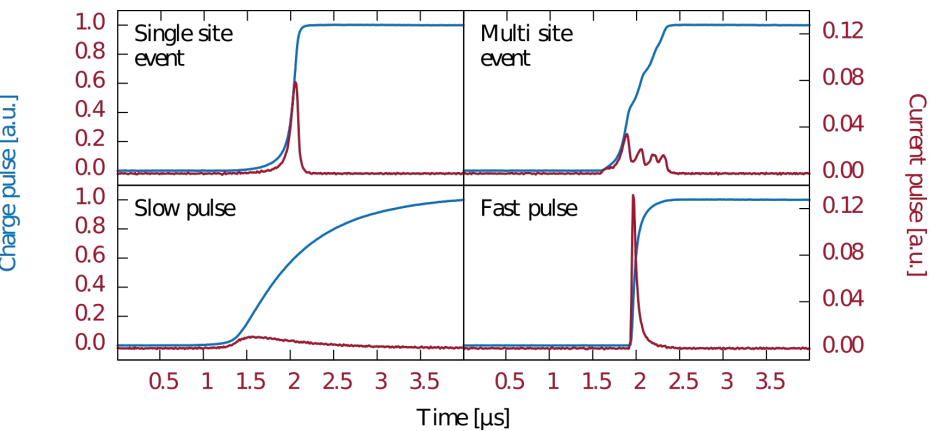
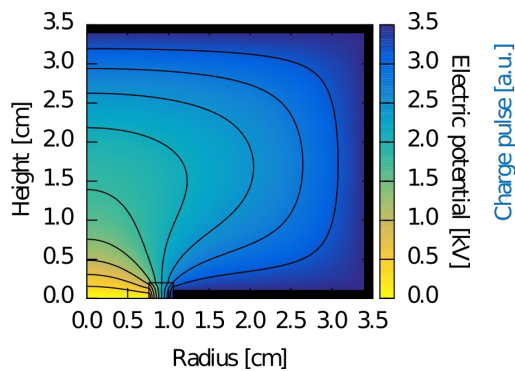
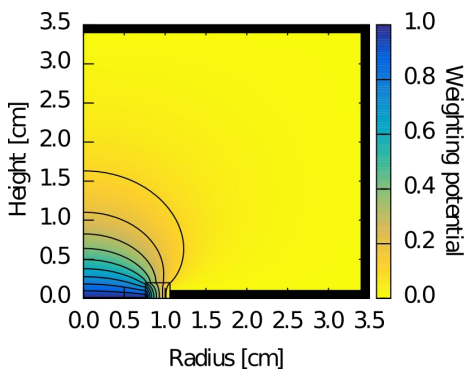
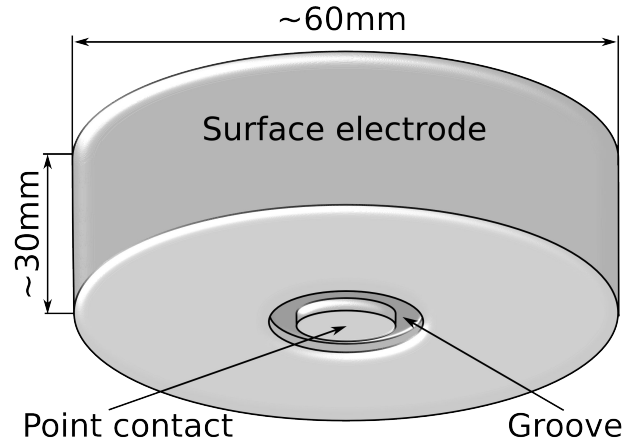
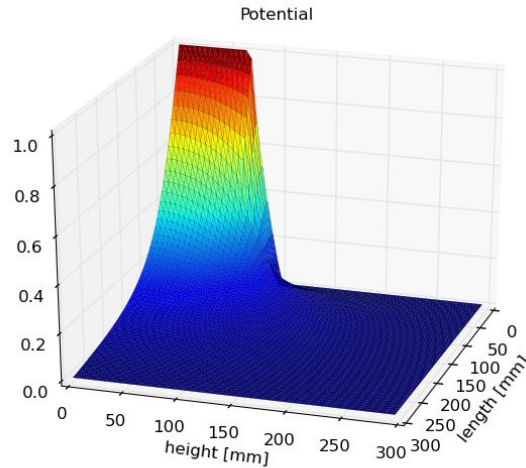
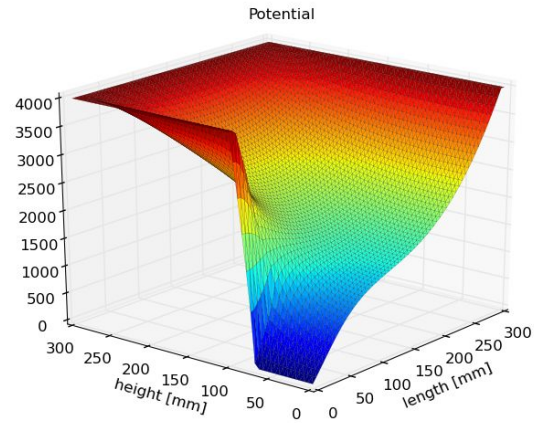


Tangential anisotropy,

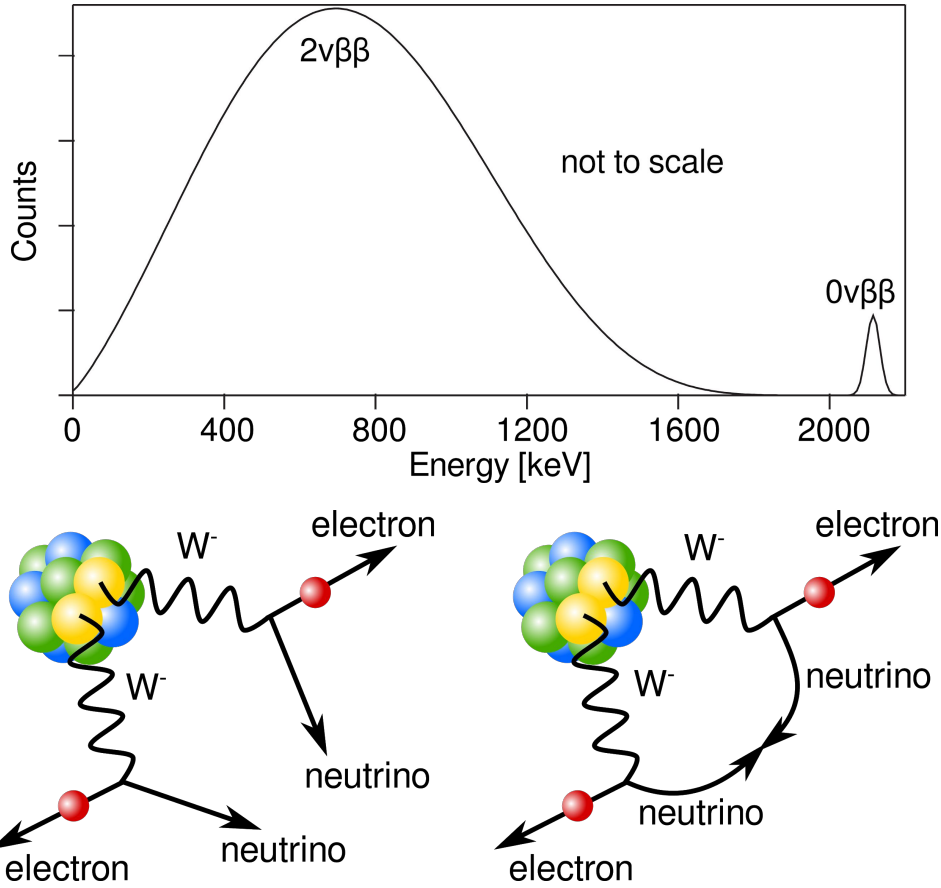
- Tangential component in drift direction if not along symmetry axis of crystal structure (otherwise symmetry would be broken by charge movement)
- Crystals pulling direction is $<100>$
- $<100>$ and $<110>$ separated by 45deg and usually in detector plane
- Faster drift along $<100>$, slower drift along $<110>$



Broad Energy Germanium Detectors (BEGe)



Neutrinoless double beta decay



- For some nuclide beta decay is energetically forbidden, but two simultaneous beta decays are allowed \Rightarrow Two-neutrino double beta decay: $(A, Z) \rightarrow (A, Z + 2) + 2e^- + 2\nu e$
- Most models beyond the standard model predict that also neutrinoless double beta decay is possible: $(A, Z) \rightarrow (A, Z + 2) + 2e^- - 2\nu\beta\beta$
- Has not yet been observed
- It violates Lepton number conservation by two units
- Schechter-Valle theorem: All realizations of $0\nu\beta\beta$ are connected to a Majorana neutrino mass, however, it can be very small (10^{-23} eV) and thus can not explain the mass observed in neutrino oscillation experiments

GERDA

Location

- LNGS (Laboratori Nazionali del Gran Sasso) Italy
- Highway tunnel, 3400m.w.e.
Underground

Water tank

- 590m³ ultra-pure water
- Neutron moderator/absorber
- Muon Cherenkov veto

Cryostat

- 64m³ LAr
- Cooling medium
- Passive shielding

Phase II

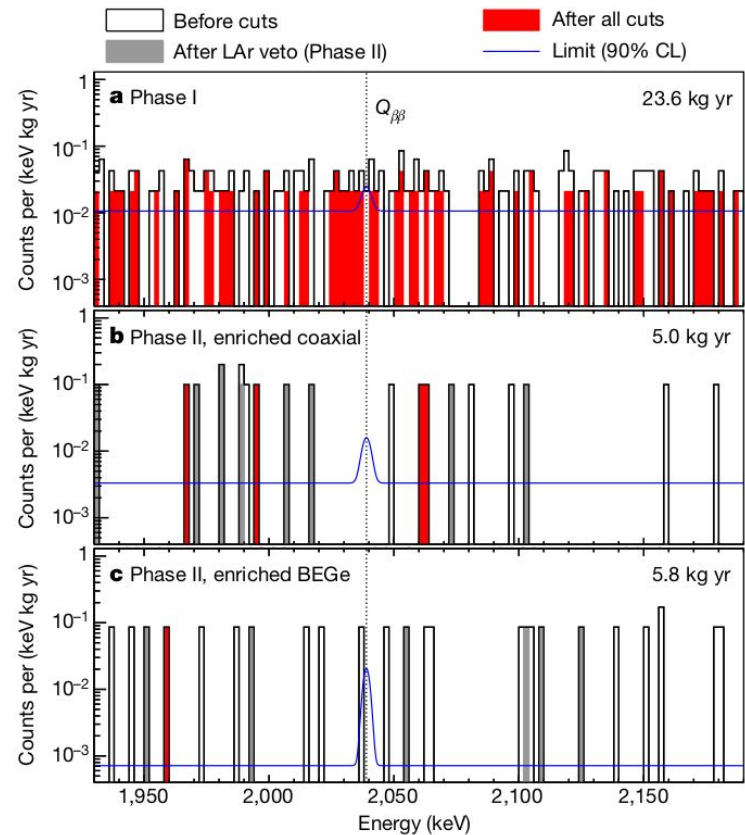
- 30 BEGe detectors/some semi-coaxial detectors



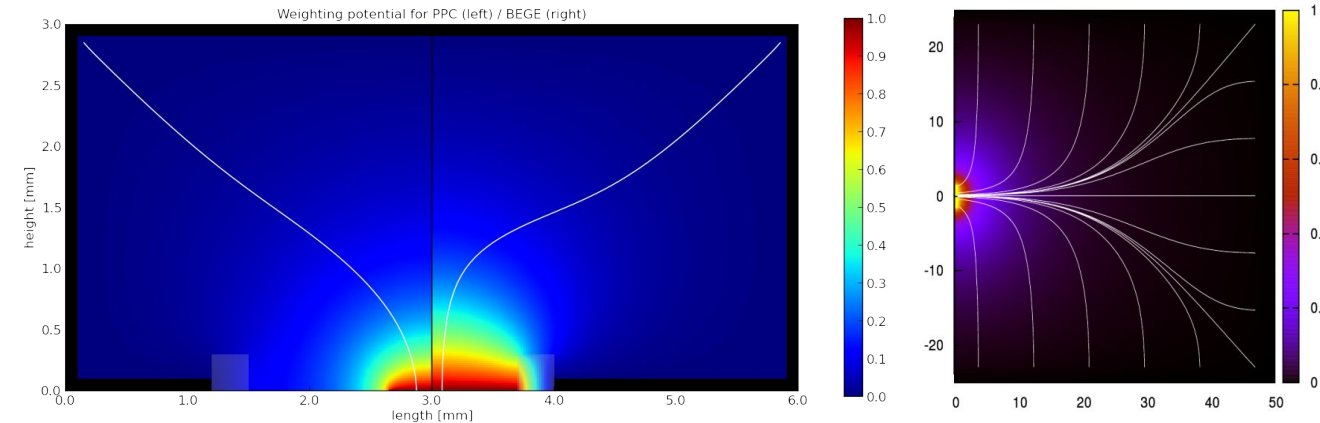
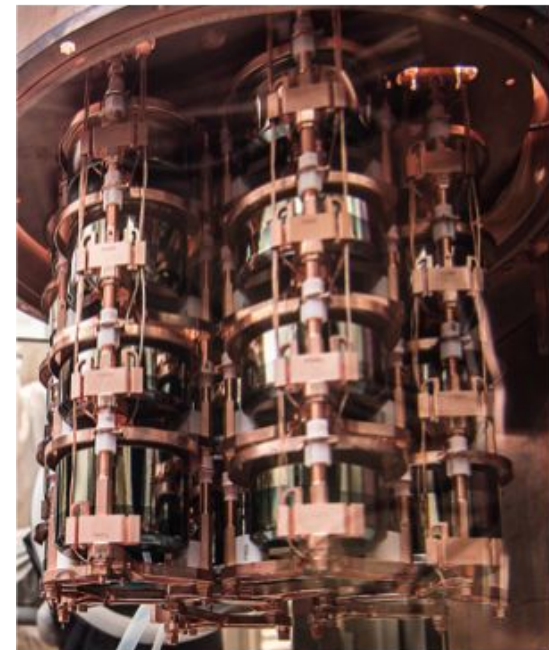
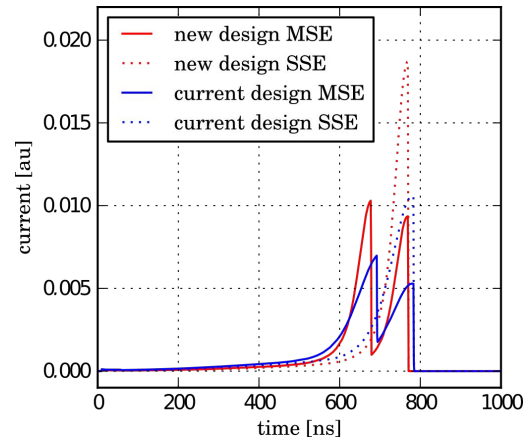
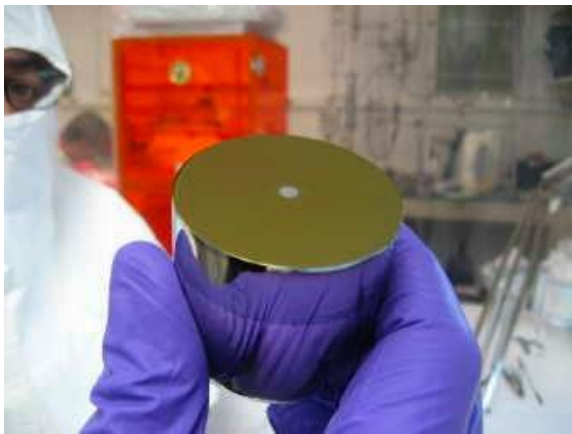
Search for extremely rare events

- Half life limit of 5.3×10^{25} yr
- Energy resolution (FWHM) of 3.2 keV at 2.6 MeV (BEGe detectors)
- Background of less than 1 event expected at $Q_{\beta\beta}(2.04 \text{ MeV}) \pm 0.5 \text{ FWHM}$
- BEGes ability to suppress background events was crucial to get there

GERDA Collaboration, Background-free search for neutrinoless double- β decay of ^{76}Ge with GERDA, Nature, 544, 47 (2017)



P-type Point Contact (PPC) detector



Paul Luke and the invention of the PPC

IEEE Transactions on Nuclear Science, Vol. 36, No. 1, February 1989

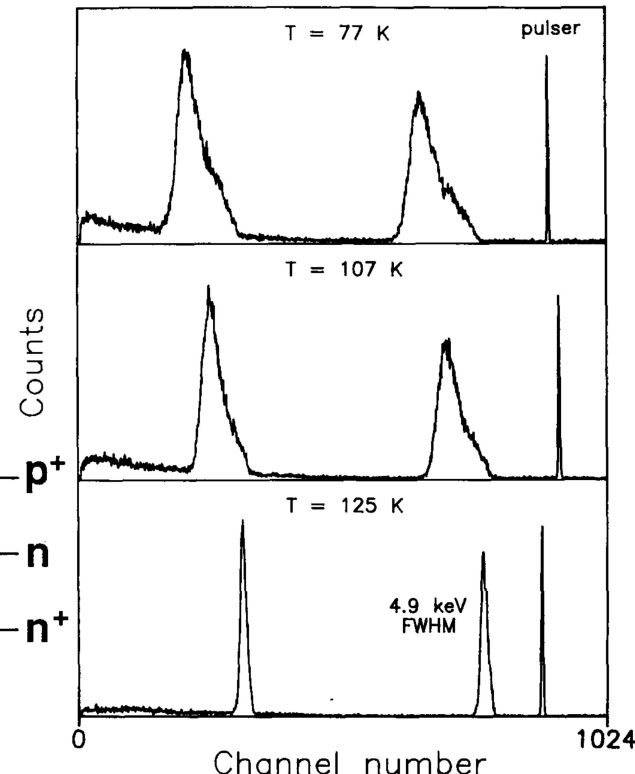
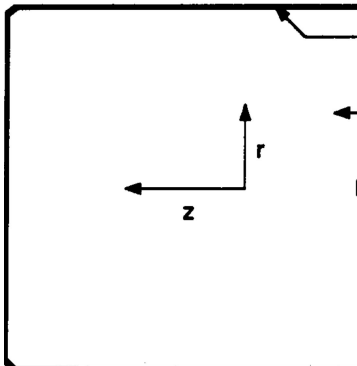
LOW CAPACITANCE LARGE VOLUME SHAPED-FIELD GERMANIUM DETECTOR

P. N. Luke, F. S. Goulding, N. W. Madden and R. H. Pehl

Engineering Division
Lawrence Berkeley Laboratory
One Cyclotron Rd.
Berkeley, California 94720 U.S.A.

Conclusion

We have successfully fabricated a large volume germanium detector with a small collecting electrode. By selecting material with the appropriate impurity concentration and gradient, a proper drift field was established inside the detector for the collection of carriers. A full depletion capacitance of $\approx 1 \text{ pF}$ was obtained. Very low noise operation is therefore possible, making such detectors good candidates for use in dark matter particle searches. For higher energy radiation, the nature of the pulse shapes obtained suggested that efficient pulse shape discrimination scheme can be implemented to distinguish between different types of radiation. We have shown that charge carrier trapping effects can be reduced by increasing the detector temperature. Further improvements may be obtained by selecting materials with higher impurity concentrations and gradients to generate higher drift fields, and by using material with lower electron trap concentrations. It may also be possible to use electronic corrections, including ballistic deficit correction [9], to improve the energy resolution.



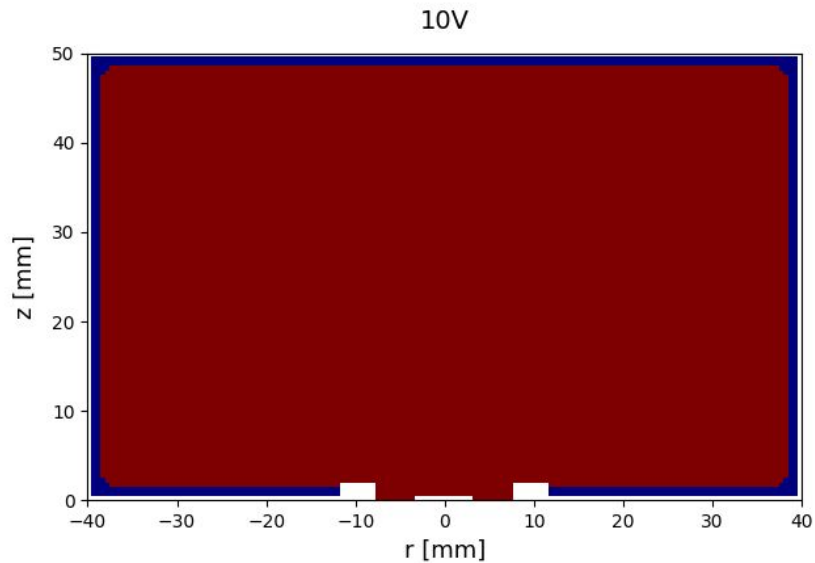
XBL 8810-3568

Structure of the shaped-field detector.

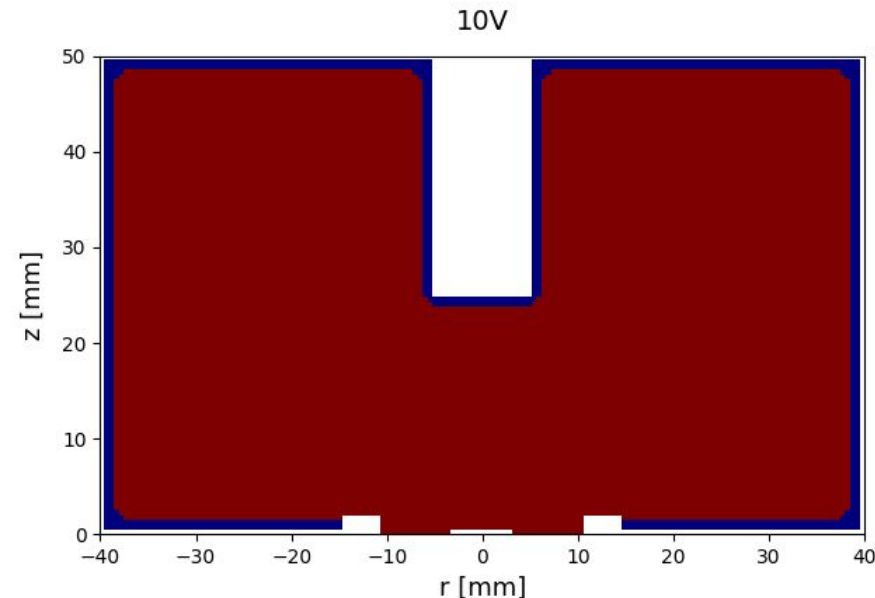
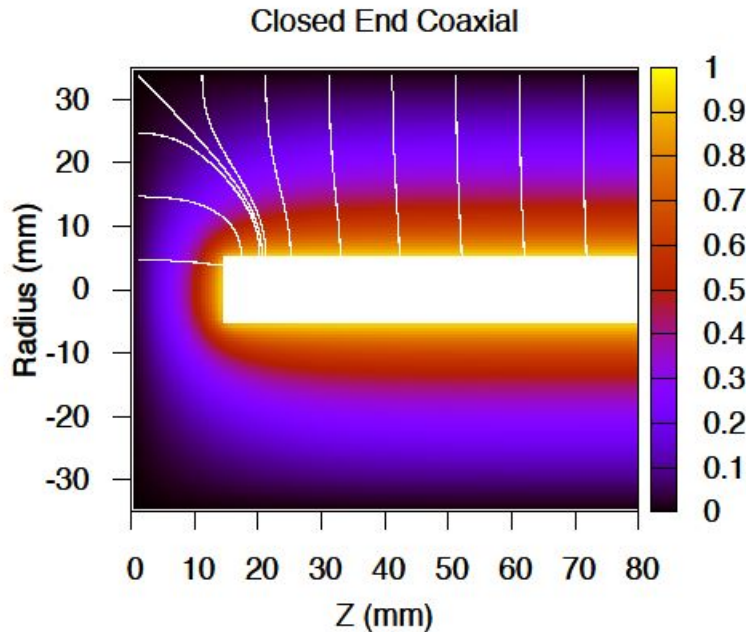
XBL 8810-3564

Limitation of BEGe/PPCs

- The average size of the BEGes in GERDA is 0.66 kg.
- The average size of the PPCs in MJD is 0.85 kg.
- If we had larger detectors, we could have fewer detector holders, cables, front ends, ...
- We might also find other application in nuclear structure, ...
- So why are PPCs and BEGes so small?
 - Required maximum depletion voltages
 - Required minimum electric field strength
 - Too low a field can lead to charge trapping and poor resolution



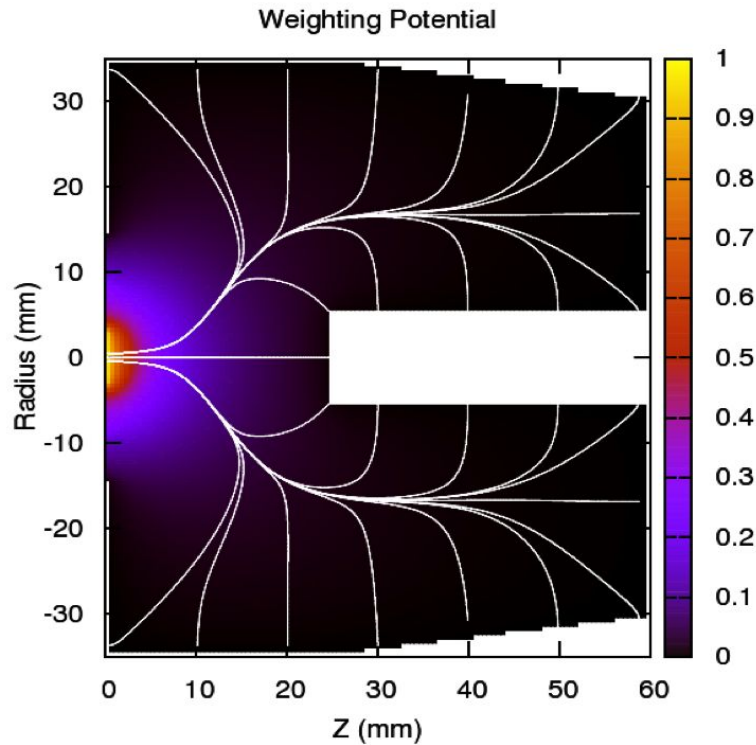
Inverted Coaxial Point Contact detector



- Much larger volume at much lower depletion voltage
- Same small contact, low capacitance and threshold as a PPC or BEGe
- Same or better PSA for Single Site / Multi Site Event discrimination
- Very unusual drift paths (long drift time, degrades energy resolution slightly)

Tuning the Geometry

- For a given impurity profile:
- Crystal length (and diameter)
- Well depth
- Li (ditch) diameter
- P+ contact diameter
- Tapering
- Improves longitudinal field beside the hole
- Outside
- Inside hole (Removes a lot less material)
- Multiple prototypes around, design for next generation ton-scale experiment (LEGEND)



Recaps

General

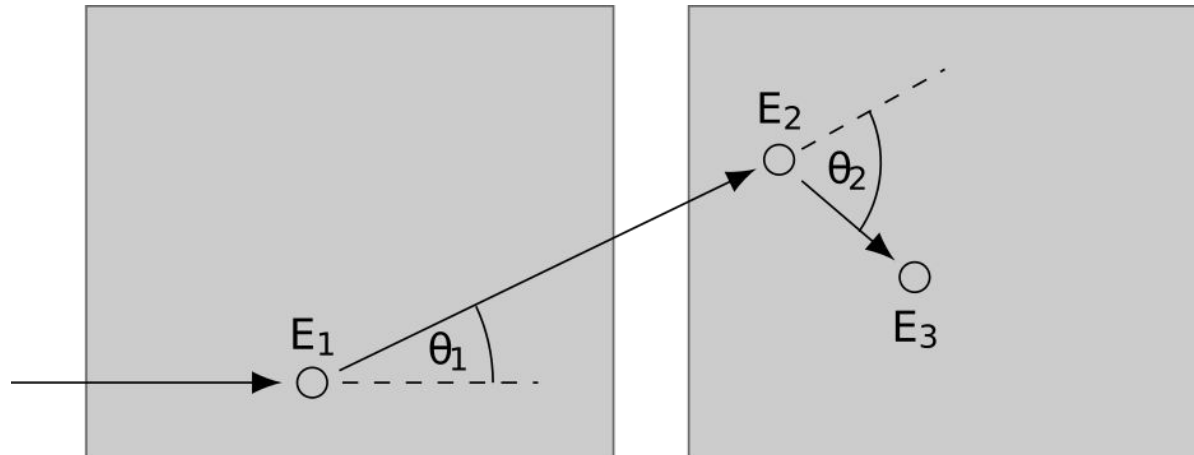
- Zone refining for purification
- Crystal pulling defines crystal axes and symmetries
- Bulk material either n-type or p-type, depending on application
- Lithium diffusion for n-type contact, boron implantation for p-type contact

BEGE/PPC detectors

- Weighting field confined to point contact, allowing pulse shape discrimination
- Excellent energy resolution, perfect for search of rare events
- Inverted coaxial geometry furthermore enables large volume detectors

Compton scattering and segmentation

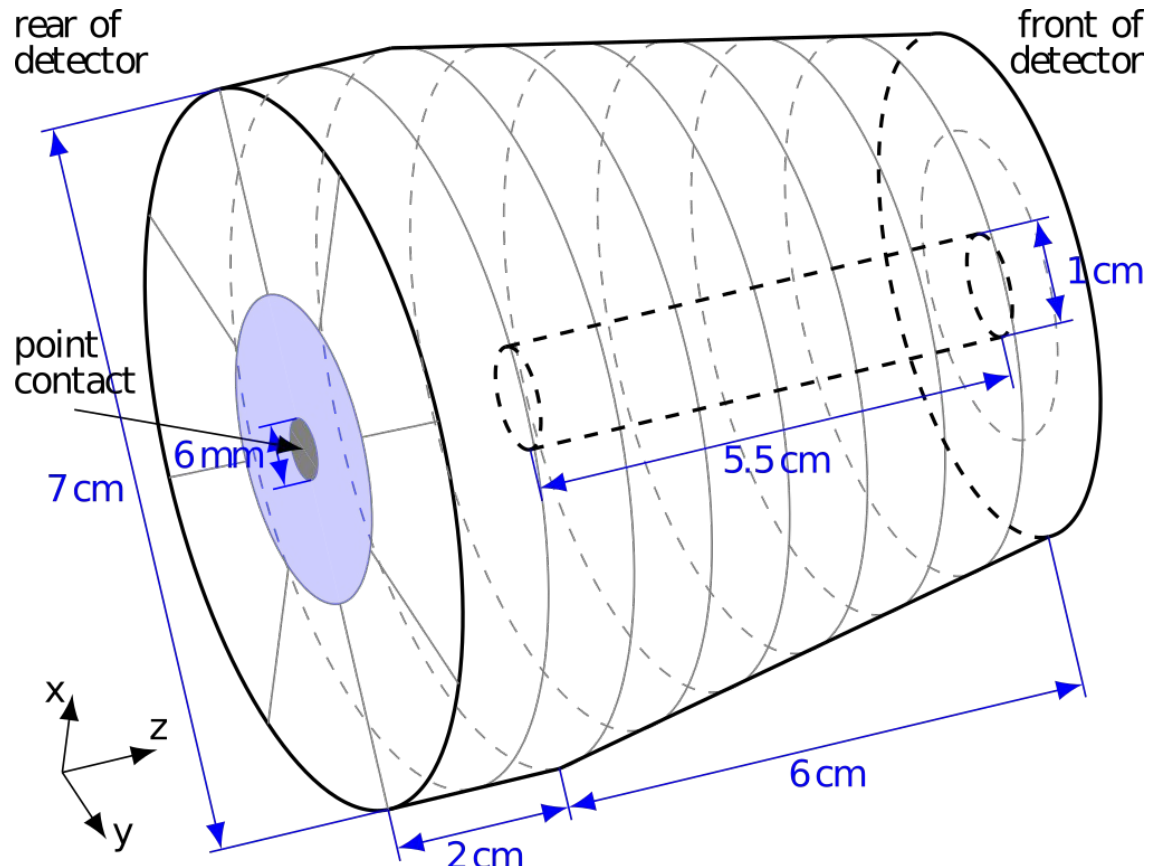
- Between ~ 100 keV and a few MeVs Compton scattering is the dominate interaction of gamma-rays in germanium
- Compton scattering equation: $E' = E/(1 + E(1 - \cos \theta)/mc^2)$
- Knowing interaction positions and deposited energy allows to reconstruct track and thus total energy of initial gamma-ray
- Adding segmentation to inverted coaxial point-contact detector allows for gamma-ray interaction position reconstruction
- Full charge collection vs image charge indicates proximity to segment



Segmented inverted coaxial point contact detector

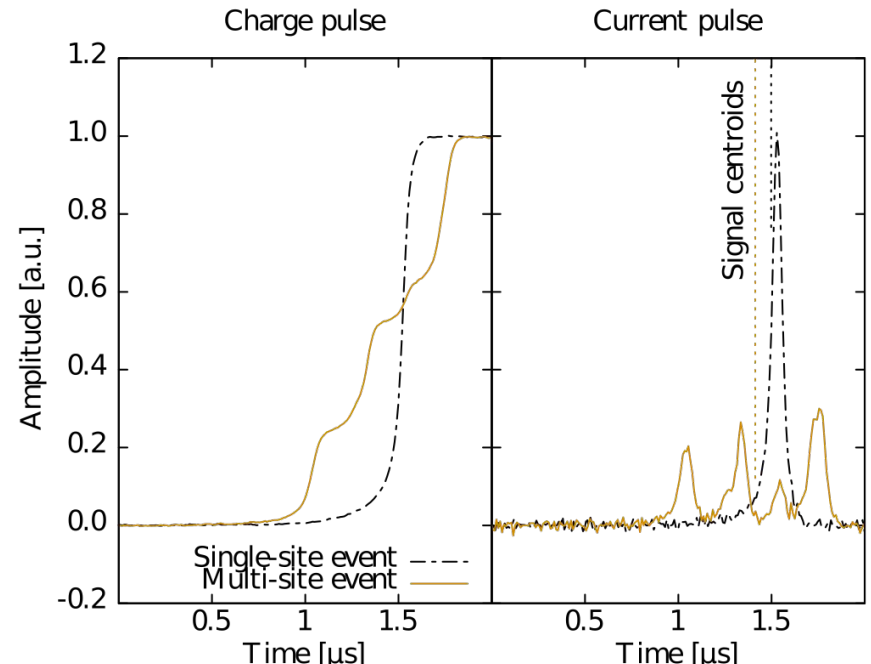
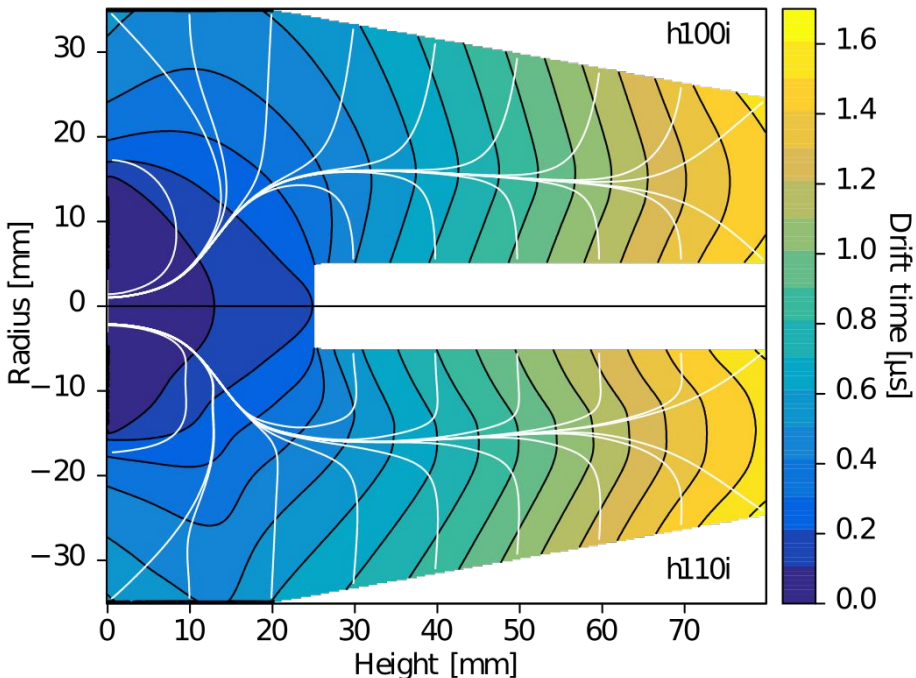
20 individual segments

- Point contact (central electrode) on the back
- 8 wedges surrounding the point contact
- 8 longitudinal circular segments on the side
- 2 concentric circular segments on the front
- 1 segment in the bore hole
- First segmented prototype delivered to D. C. Radford (ORNL) in 2012



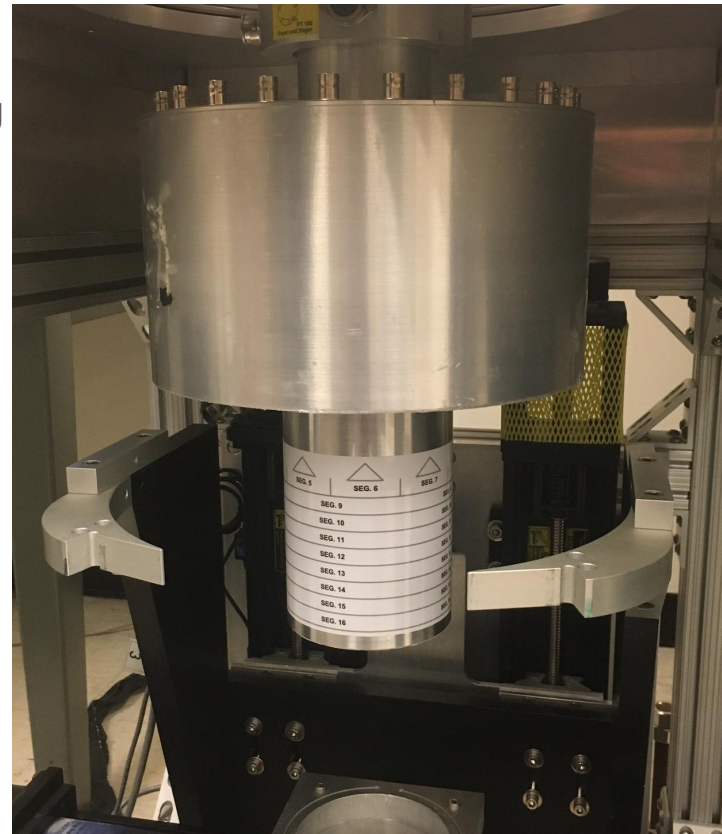
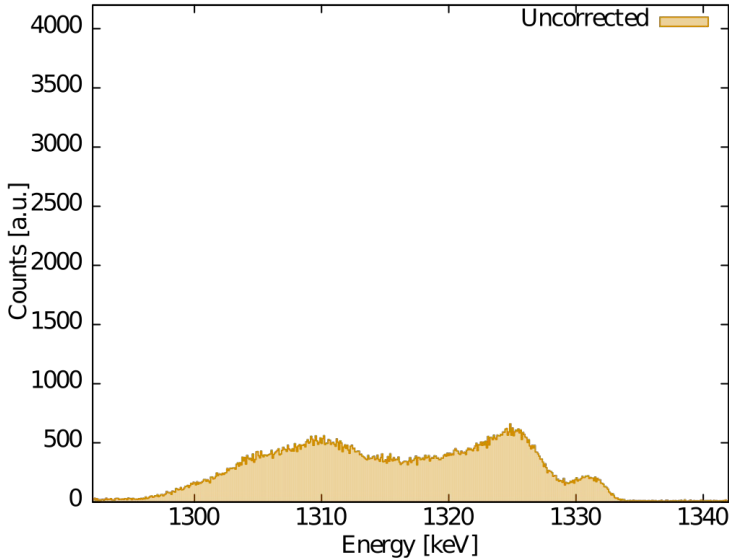
Detector properties

- Majority charge carries (electrons) drift through detector to be collected at the point contact
- Strong variation in charge drift time (a few 100 ns to 2 μ s), similar charge collection trajectories and a highly localized point contact weighting potential allows direct identification of number of interactions
- The charge drift time is a proxy for the z-position (height) of an interaction



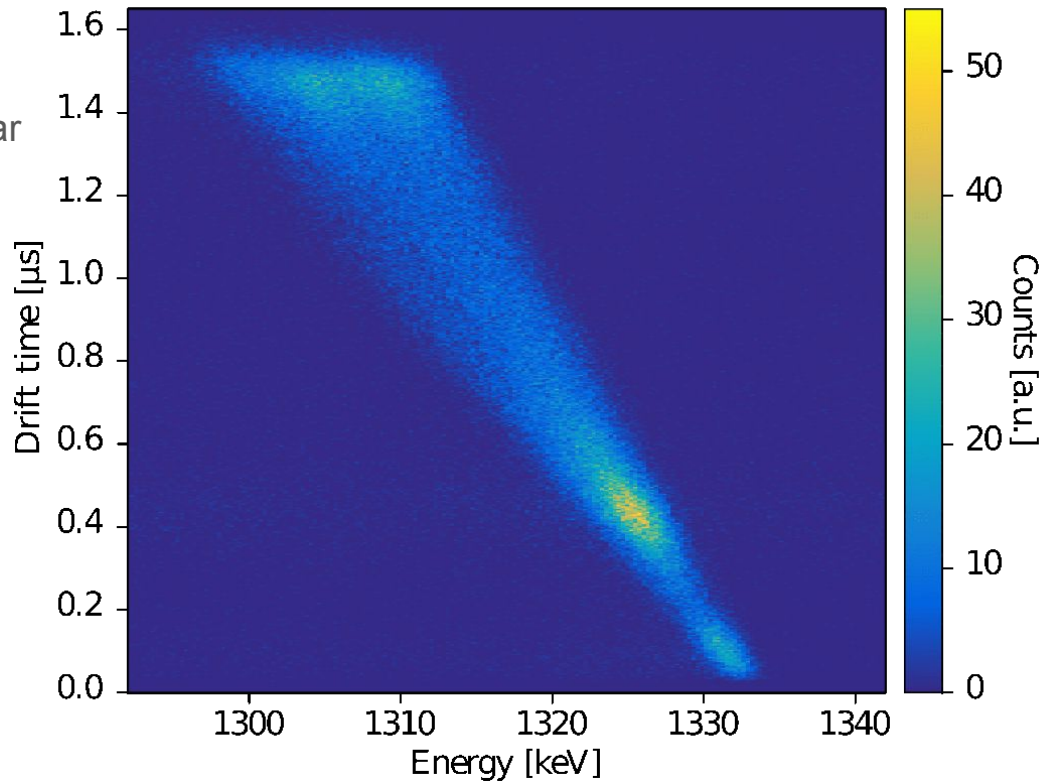
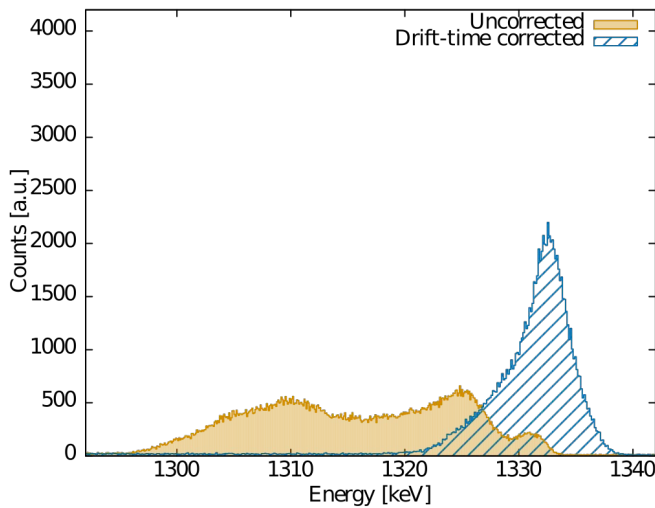
Prototype detector from ORNL at LBL

- For n-type material trapping is significant even at standard impurity levels (without damage)
- Large variation in drift times/paths and the associated trapping strongly degrades the resolution (and peak shape)
- Example: 1332.5 keV transition of uncollimated ^{60}Co source centered in the front of the detector (~4 inch distance)



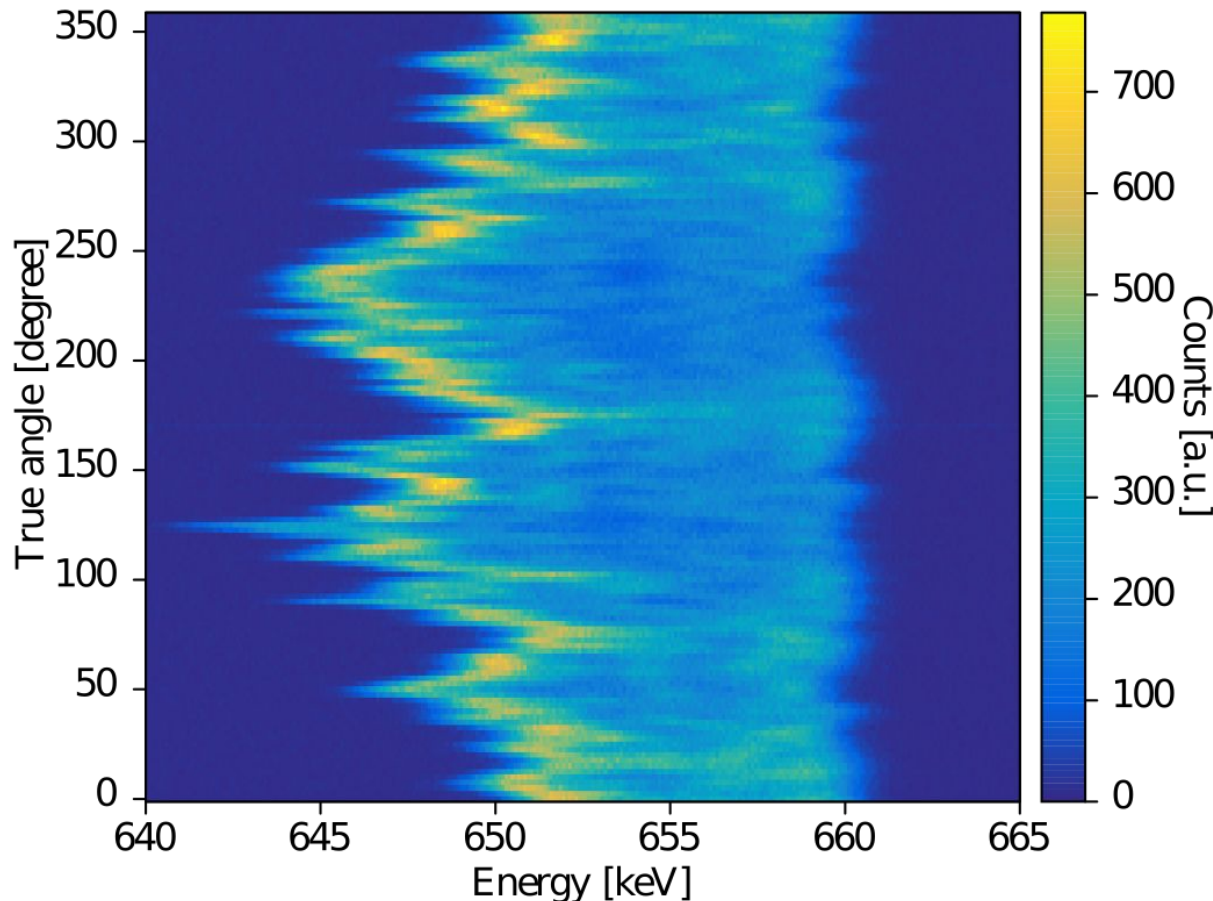
Drift time correction

- To a first approximation, charge trapping increases linearly with drift time
- Divide data into (100ns) drift-time slices
- Calculate centroid in each slice to find linear correction
- Correct energy according to drift time correction curve



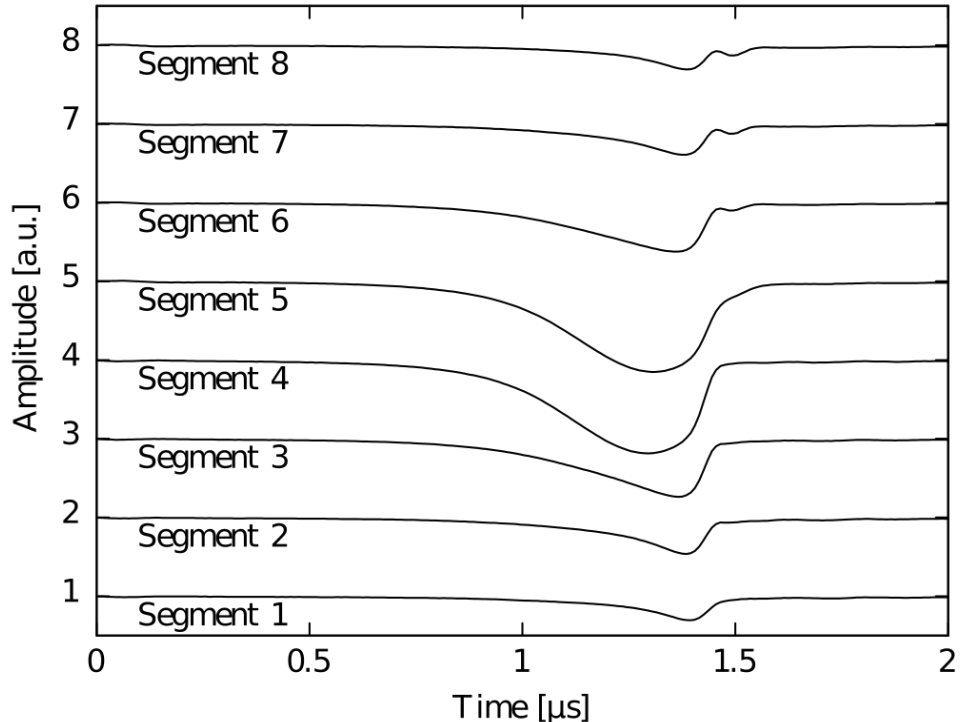
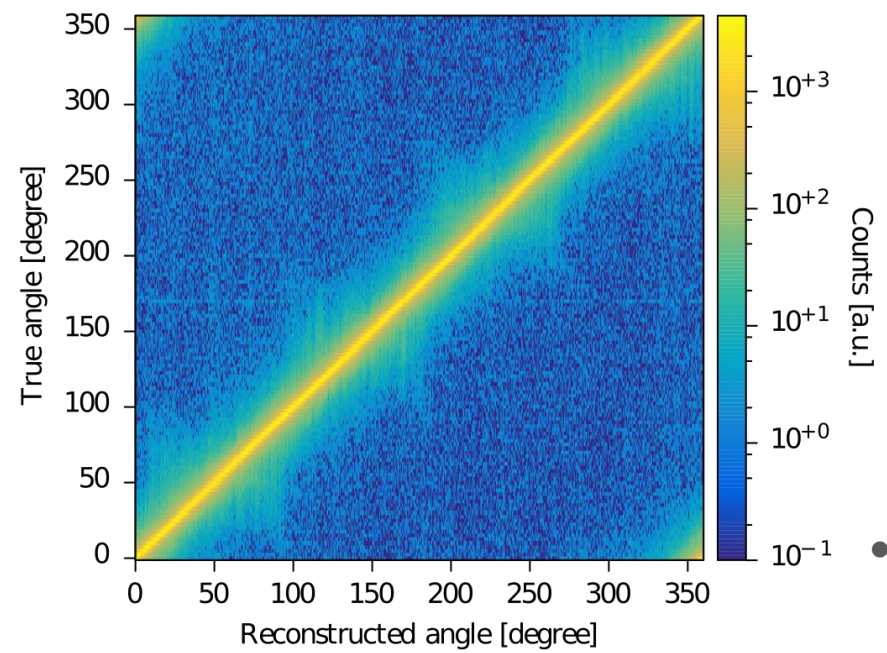
Additional correction: Azimuthal dependence

- Collimated ^{137}Cs measurement along a ring with 24 mm radius, 2.5deg spacing between measurements
- Strong variation in the amount of trapping is clearly observed at different azimuthal angle
- Correction would require reconstruction of azimuthal angle for each individual event



Azimuthal reconstruction

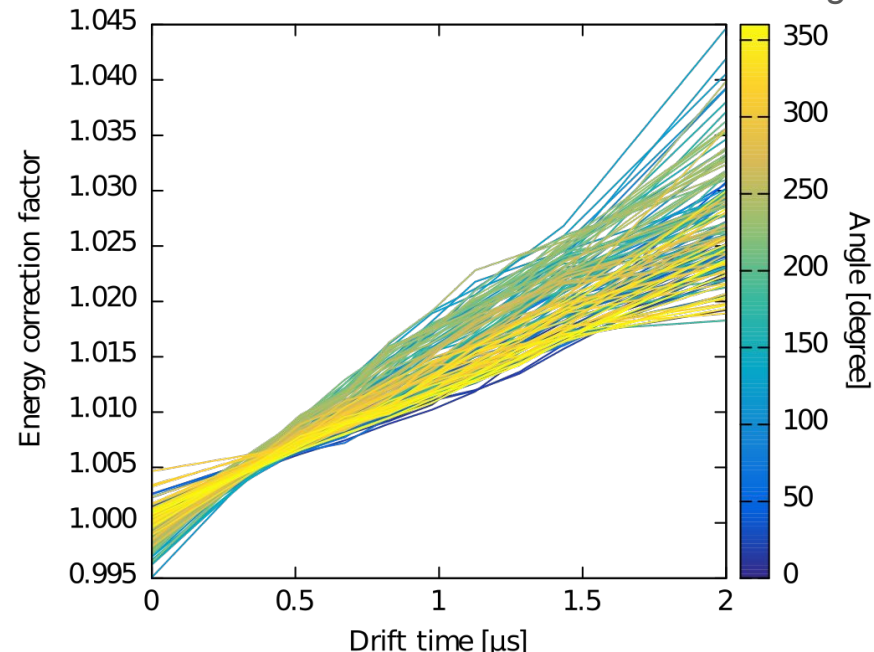
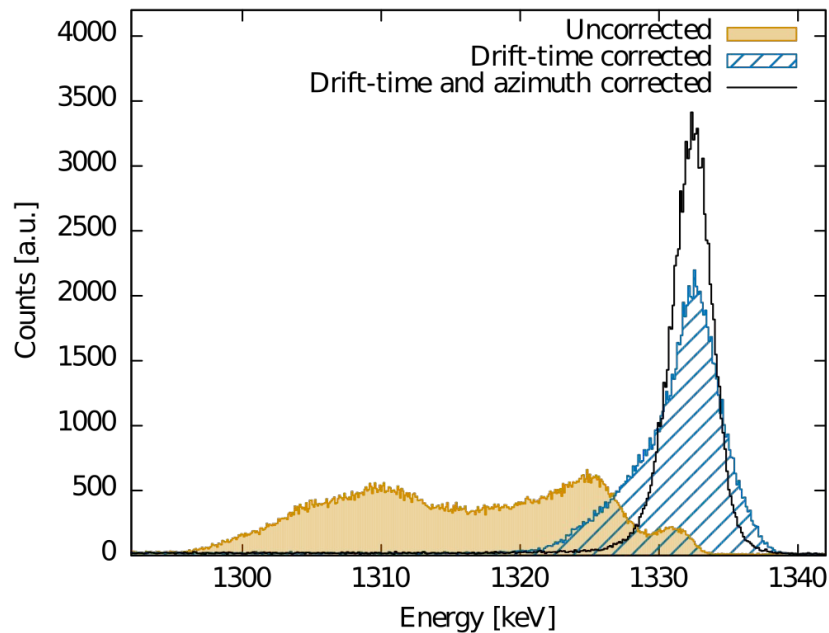
- Build an experimental basis for the 8 wedge segments on the rear of the detector based on image charges only



- Event based reconstruction by fitting of individual events to the available basis signals, using a χ^2 minimization, and a linear interpolation between grid points allows a reliable azimuthal angle determination

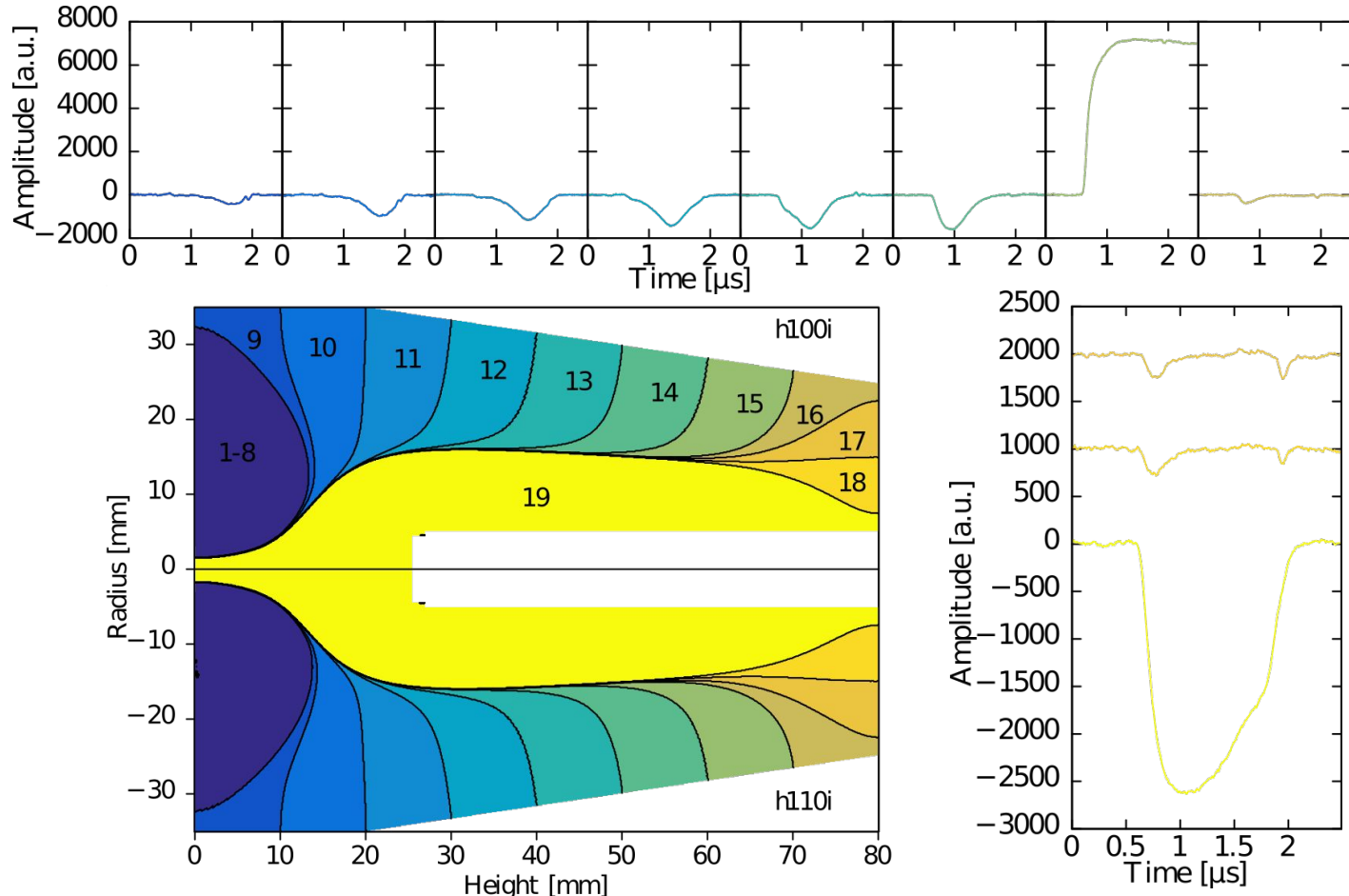
Azimuthal energy correction

- Collimated vertical ^{137}Cs measurements were taken along a ring with 24 mm radius, with 2.5deg spacing between measurements
- Drift time correction curves were determined for each angular position variation is significant, several percent deviation between correction curves
- These curves are used to correct the energy of an individual event as a function of it's drift time and angle



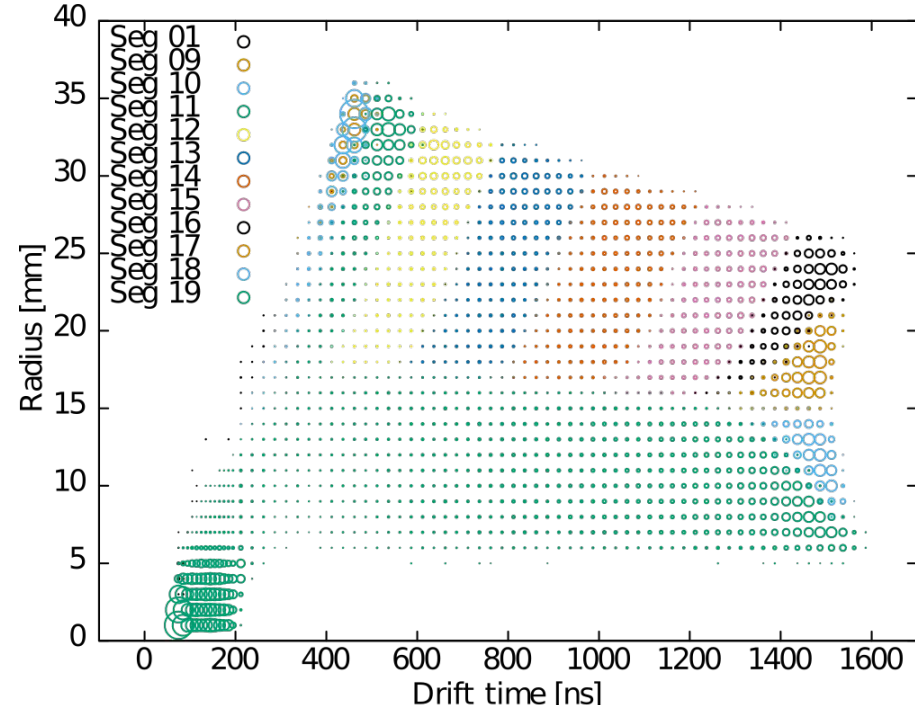
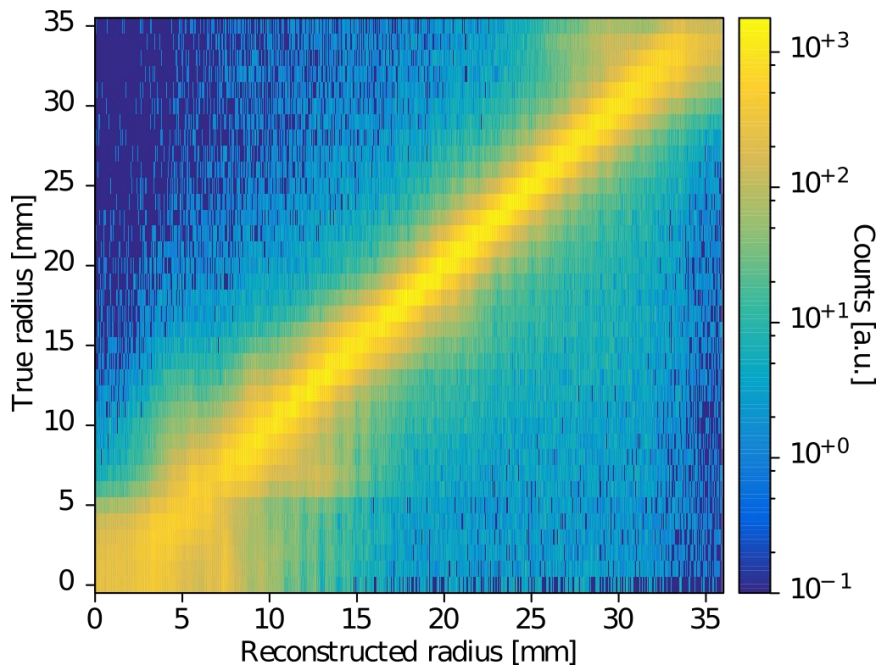
Radial reconstruction

- Drift time as proxy for z
- Angle from azimuthal reconstruction
- Remaining coordinate: radius
- Most important information for radius on segment 9-19 (side, front, bore hole)

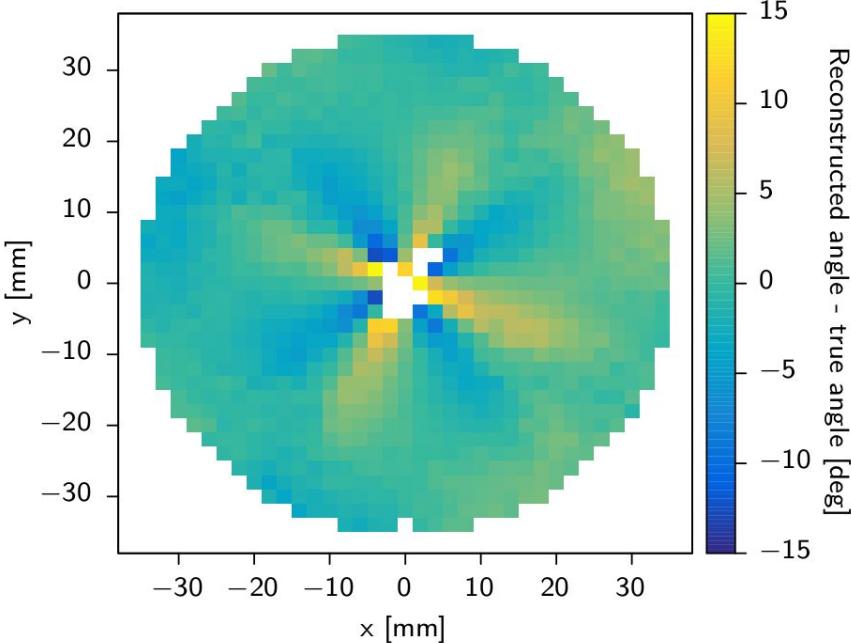
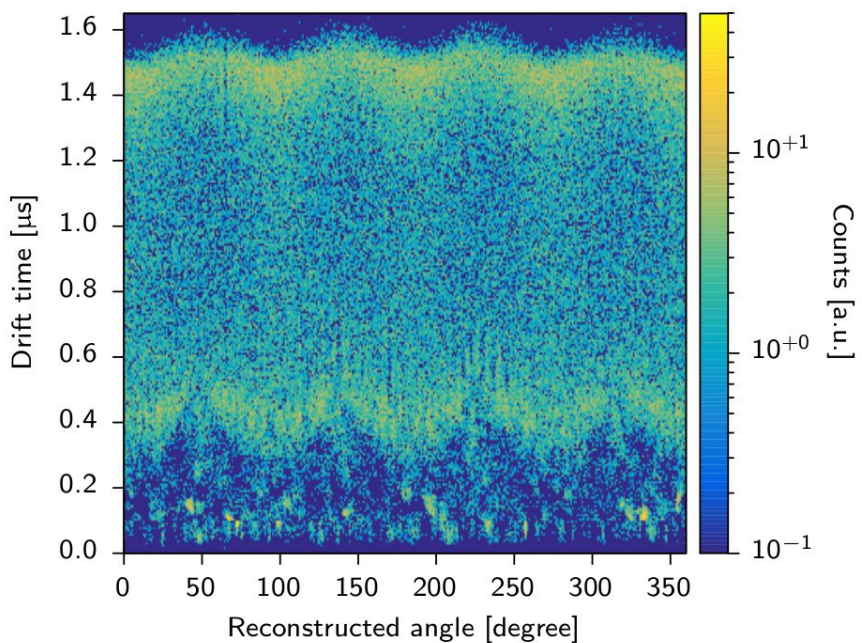


Building a radial basis

- New measurement: Collimated ^{137}Cs measurement covering a range of 45deg (size of one wedge on back), roughly 1 mm distance between points
- Assumption: Rest of angles can be projected onto that range
- Hundred of basis points a one given angle, calculate chi2 between every event and every single one of them



Angular effects



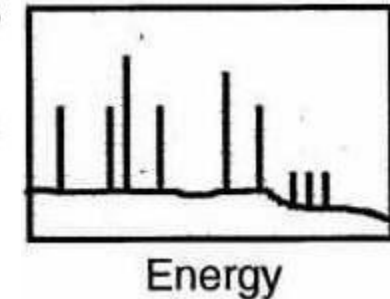
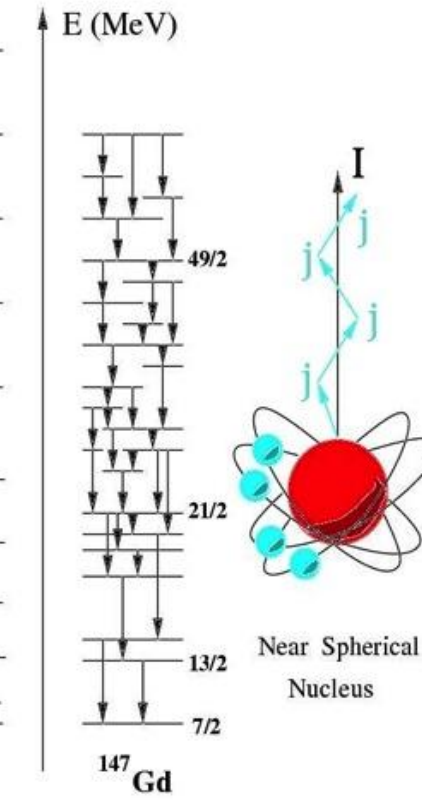
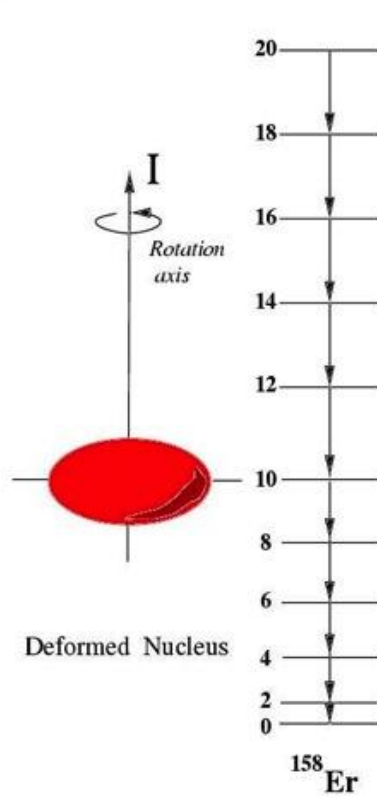
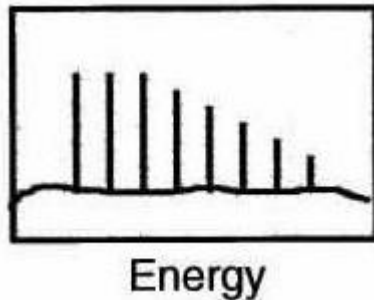
- Event reconstruction allows to study crystal lattice effect on drift direction and velocity
- Slow and fast drift along $<100>$ and $<110>$ respectively
- Tangential component if not along symmetry axis

Recaps

- 20 individual segments, each producing a signal that is digitized and processed for energy reconstruction and position reconstruction
- Segmentation gives crude position information
- Central contact measures full charge for every event, one segment measures full charge as well, remaining segments observe image charges
- Intuitive understanding of dependence between observed signals and interaction location
- 3D reconstruction of every individual events, more complex for events with multiple simultaneous interactions
- Radial reconstruction already relative complex with hundreds of basis points at each angle

Nuclear Structure Physics and Germanium detectors

- “Effective” Energy resolution
 - Doppler broadening
 - Position resolution
- Peak-to-Total
- Efficiency
- Auxiliary devices

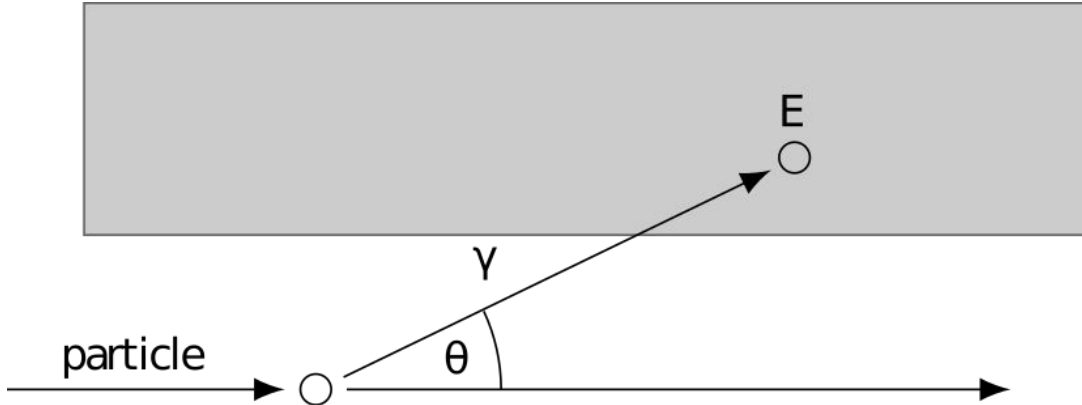


Doppler effect in high velocity beam experiments

- Gamma decay of isotope moving at highly relativistic speed with respect to the measurement frame
- Detected gamma-rays have energy shift that depends on orientation of interaction location with respect to trajectory of decaying isotope
- Considerable degradation in high velocity in-beam experiments, much more difficult to distinguish gamma-ray lines (often hundreds of them in a simple spectrum)
- The energy shift can be corrected by calculating the angle between particle trajectory and detector θ

$$E/E' = \frac{1 - \beta \cos \theta}{\sqrt{1 - \beta^2}}, \quad \beta = v/c$$

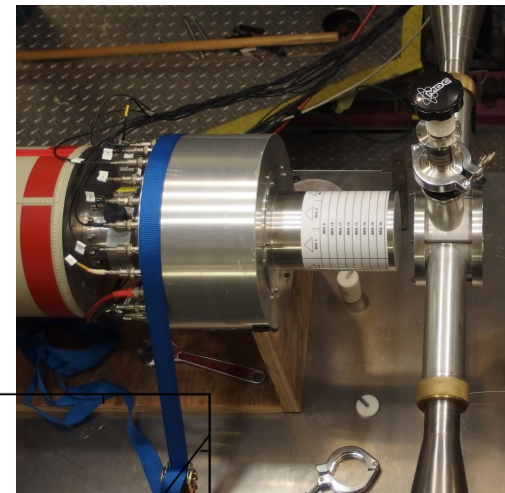
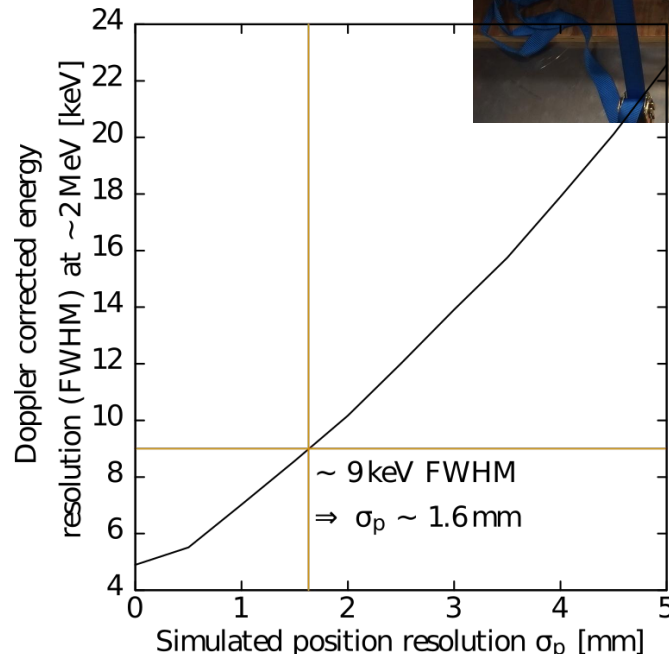
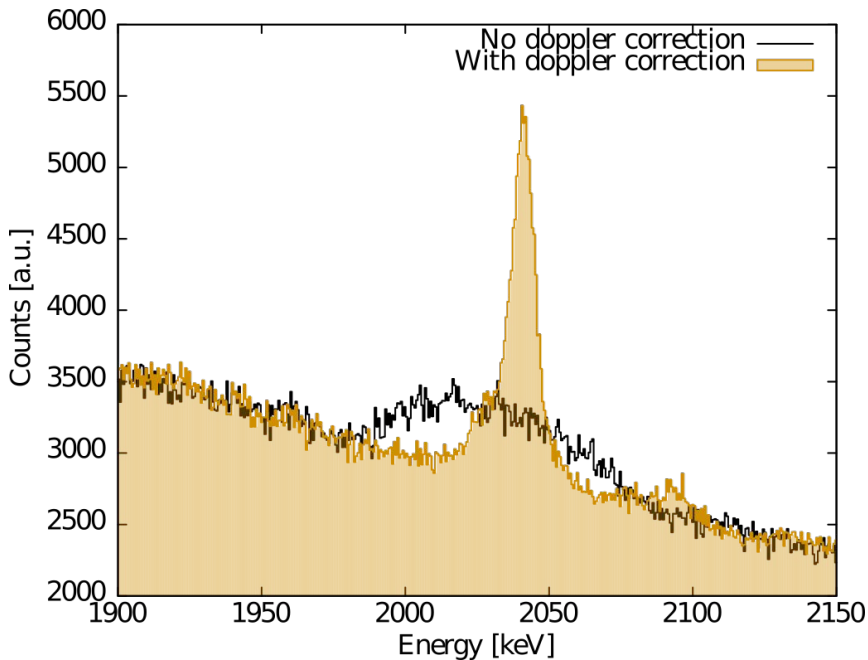
- Requires excellent position reconstruction



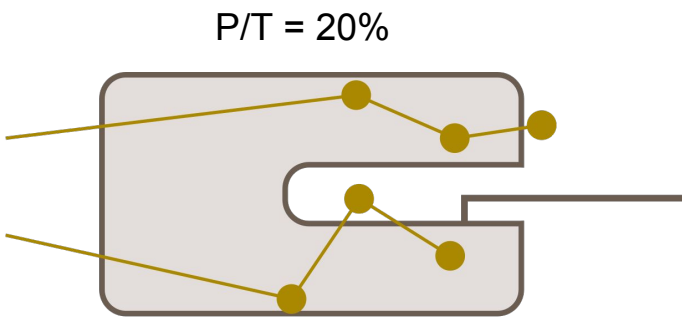
Doppler reconstruction

In Beam test at 88-inch cyclotron (Cave 4C)

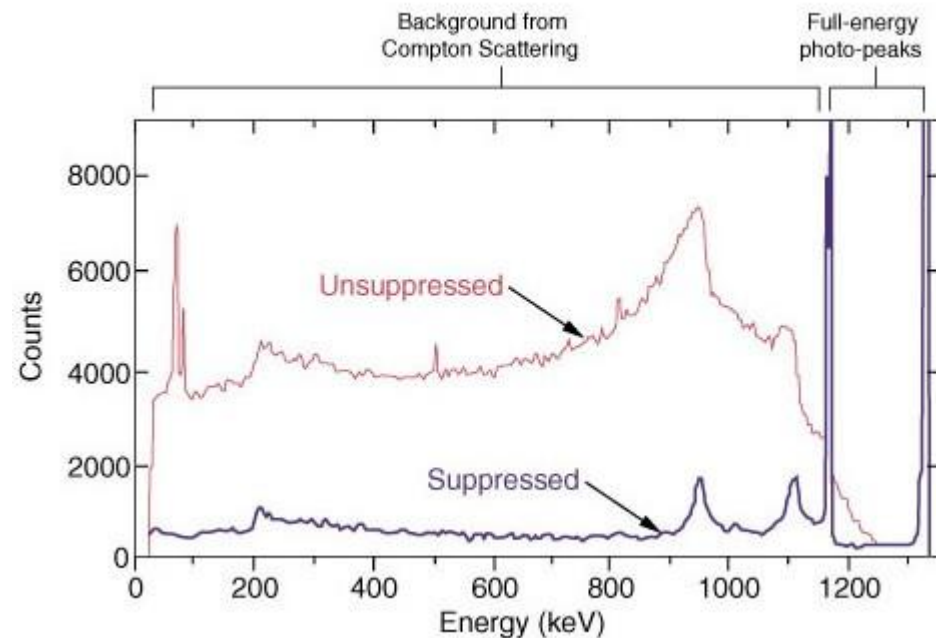
- $^{84}\text{Kr}(^{12}\text{C}, 4\text{n}) ^{92}\text{Mo}$ - ^{84}Kr at 395 MeV onto $45\mu\text{g}/\text{cm}^2$ C target
- ^{92}Mo residues recoil at $v/c \sim 0.09$
- Placement of detector within ~ 7 cm of target position allows measurement of position resolution with precision < 0.5 mm



Peak to Total: Compton Suppression

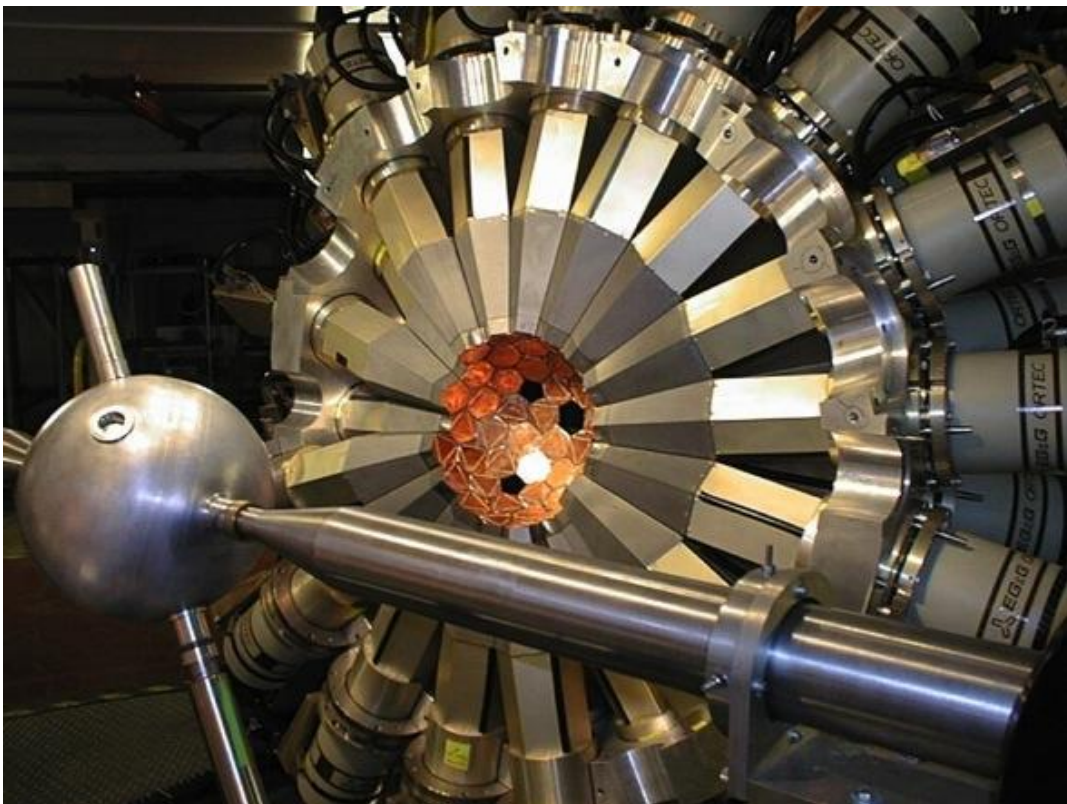


Veto by
Compton suppressor



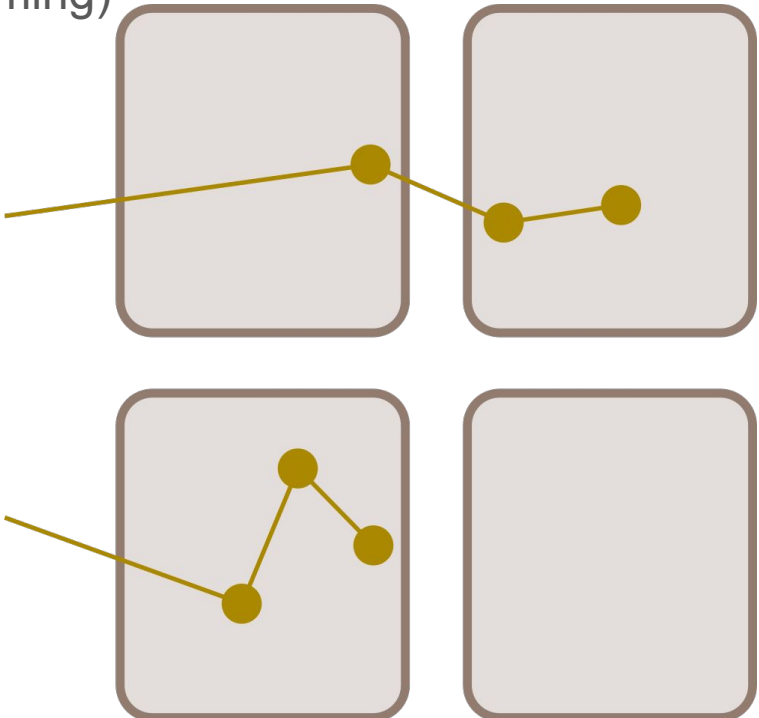
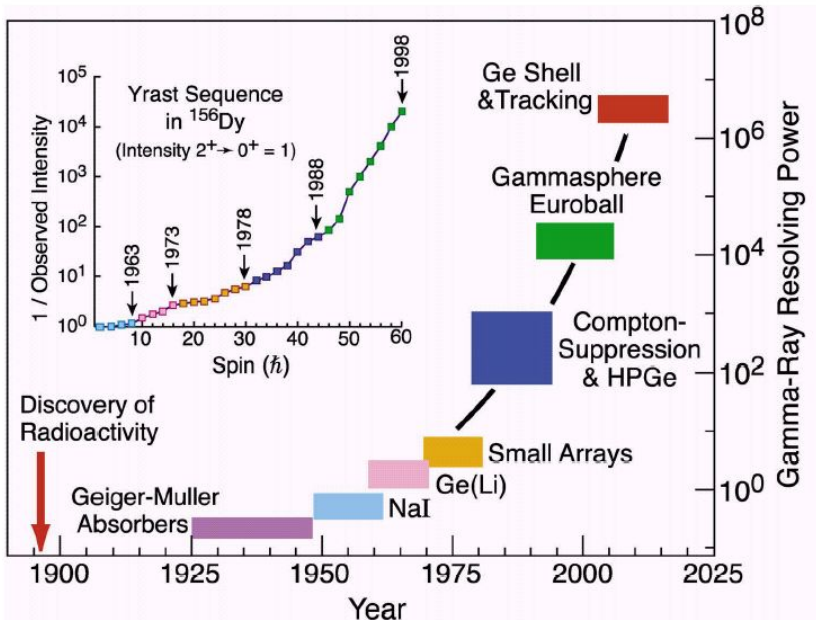
Gammasphere (since 1995)

- Number of modules: 110
- Ge Size: 7cm (D), 7.5cm (L)
- Distance to Ge: 25 cm
- Peak efficiency: 9% (1.33 MeV)
- Peak/Total: 55% (1.33 MeV)



Gamma ray tracking

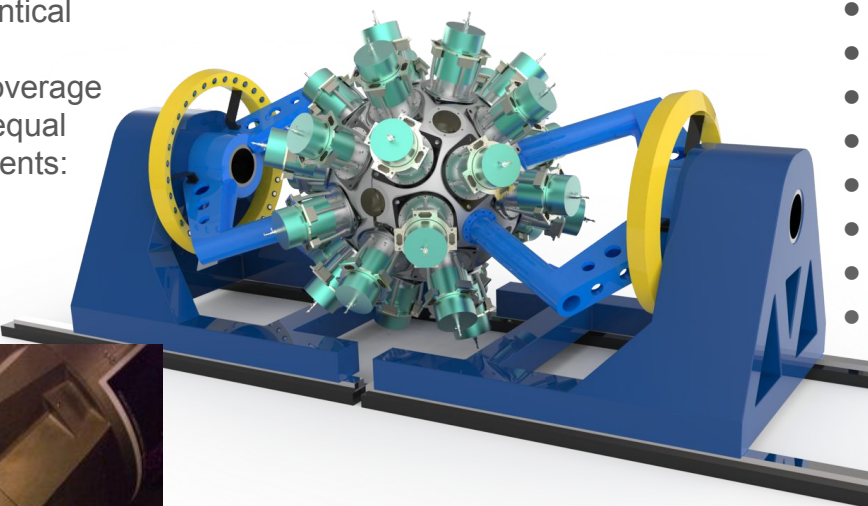
- Tracking of photon interaction points (energy and position)
- Doppler reconstruction
- Close packing of detectors (efficiency, summing)
- Peak to total



GRETINA, GRETA and AGATA

GRETINA

- Up to 48 crystal of identical shape
- $\frac{1}{4}$ of full solid angle coverage
- 4 fold clusters: 12 all equal
- Core: cold FET, segments: warm FET
- 36-fold segmentation

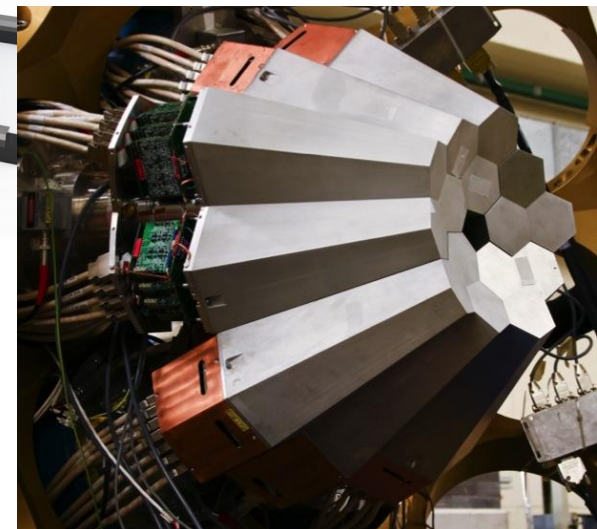


GRETA

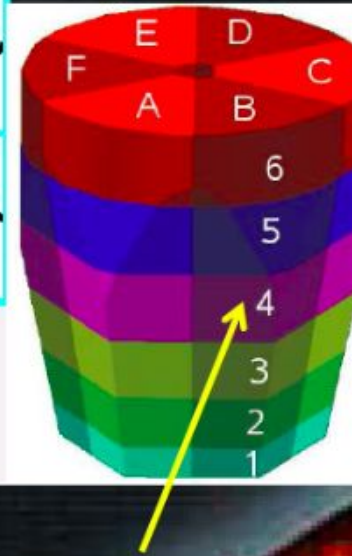
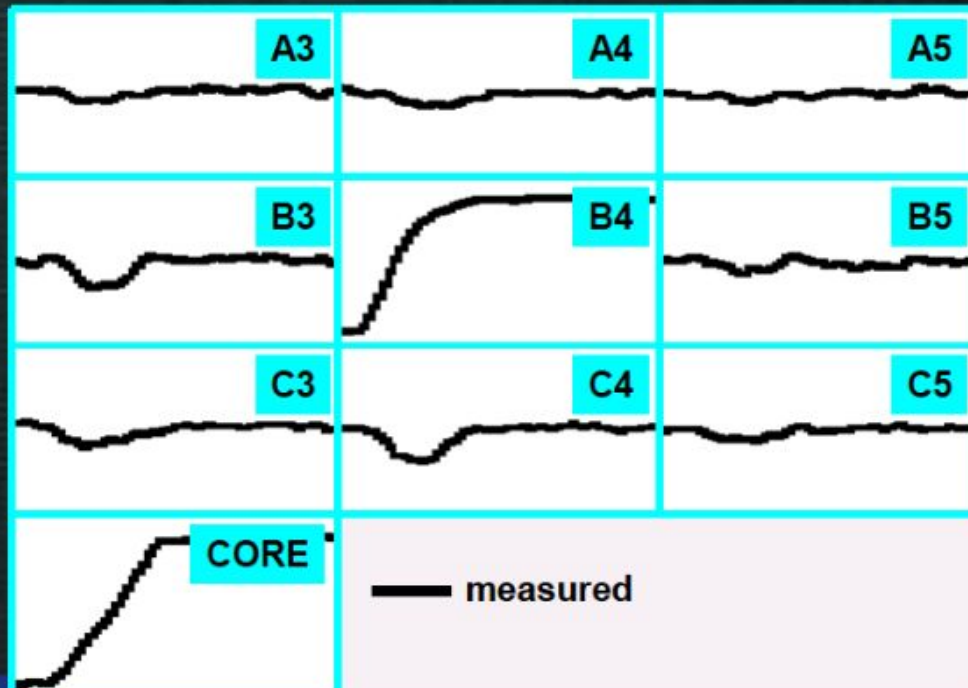
- 4PI solid angle coverage
- Peak to total of ~55%
- FRIB and ATLAS/CARIBU scientific programs will rely on GRETA
- Expected completion in 2025 when FRIB reaches full power

AGATA

- 180 hexagonal crystals: 3 shapes
- 3 fold clusters (cold FET): 60 all equal
- Inner radius (Ge): 23.5 cm
- Amount of germanium: 362 kg
- Solid angle coverage: ~82 %
- 36-fold segmentation: 6480 segments
- Crystal singles rate: ~50 kHz
- Efficiency ~43%, peak to total ~58%

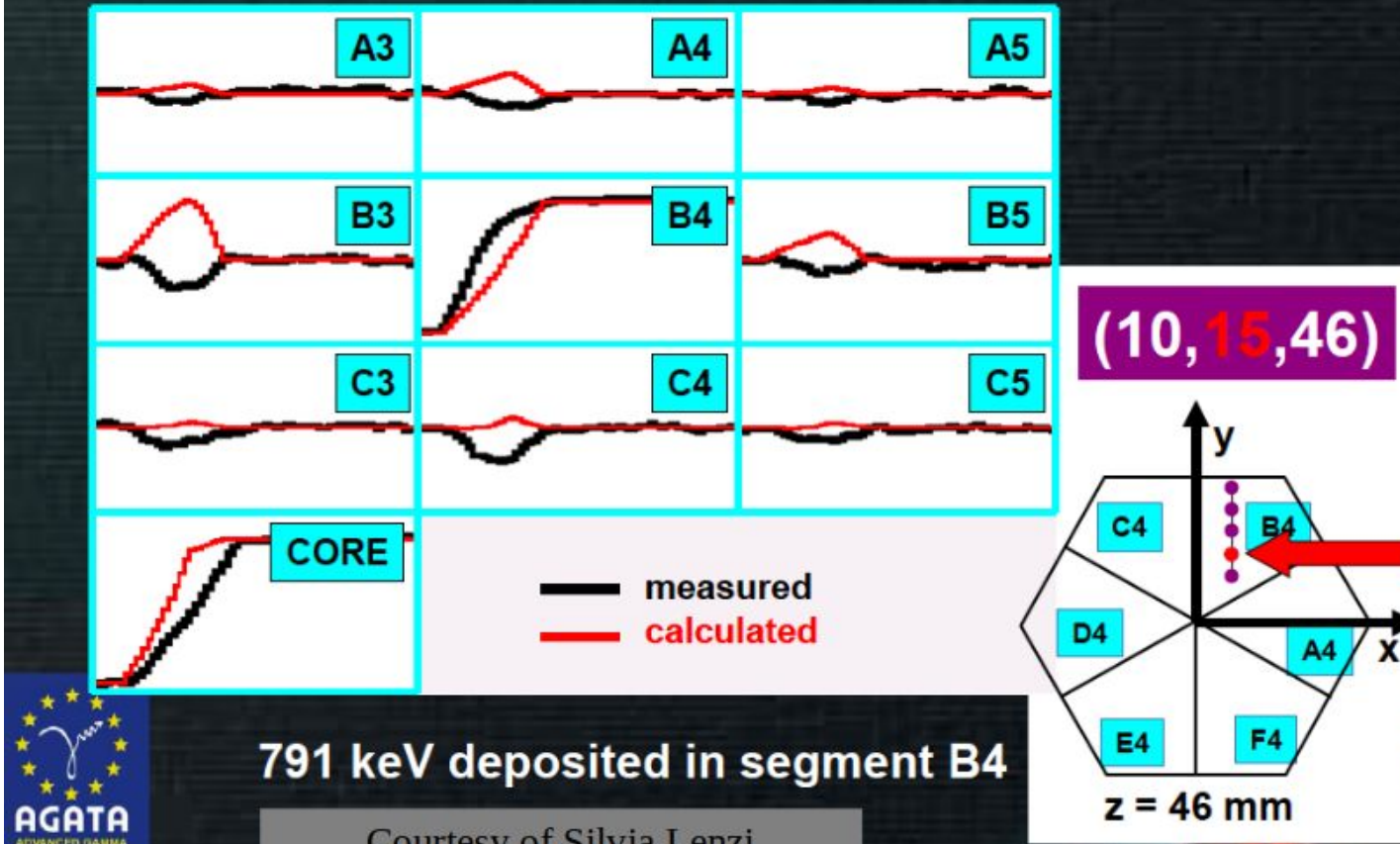


The pulse-shape analysis process

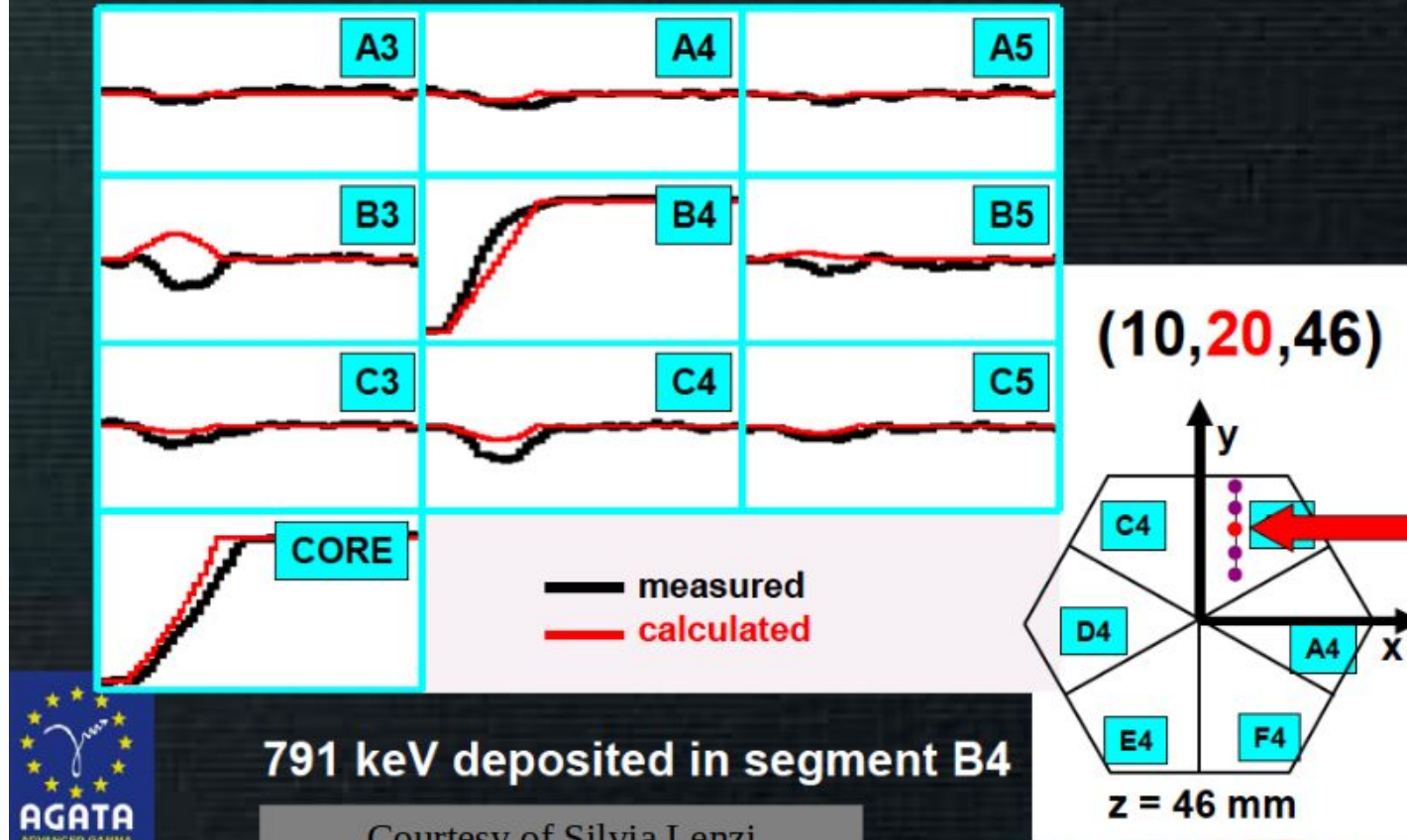


791 keV deposited in segment B4

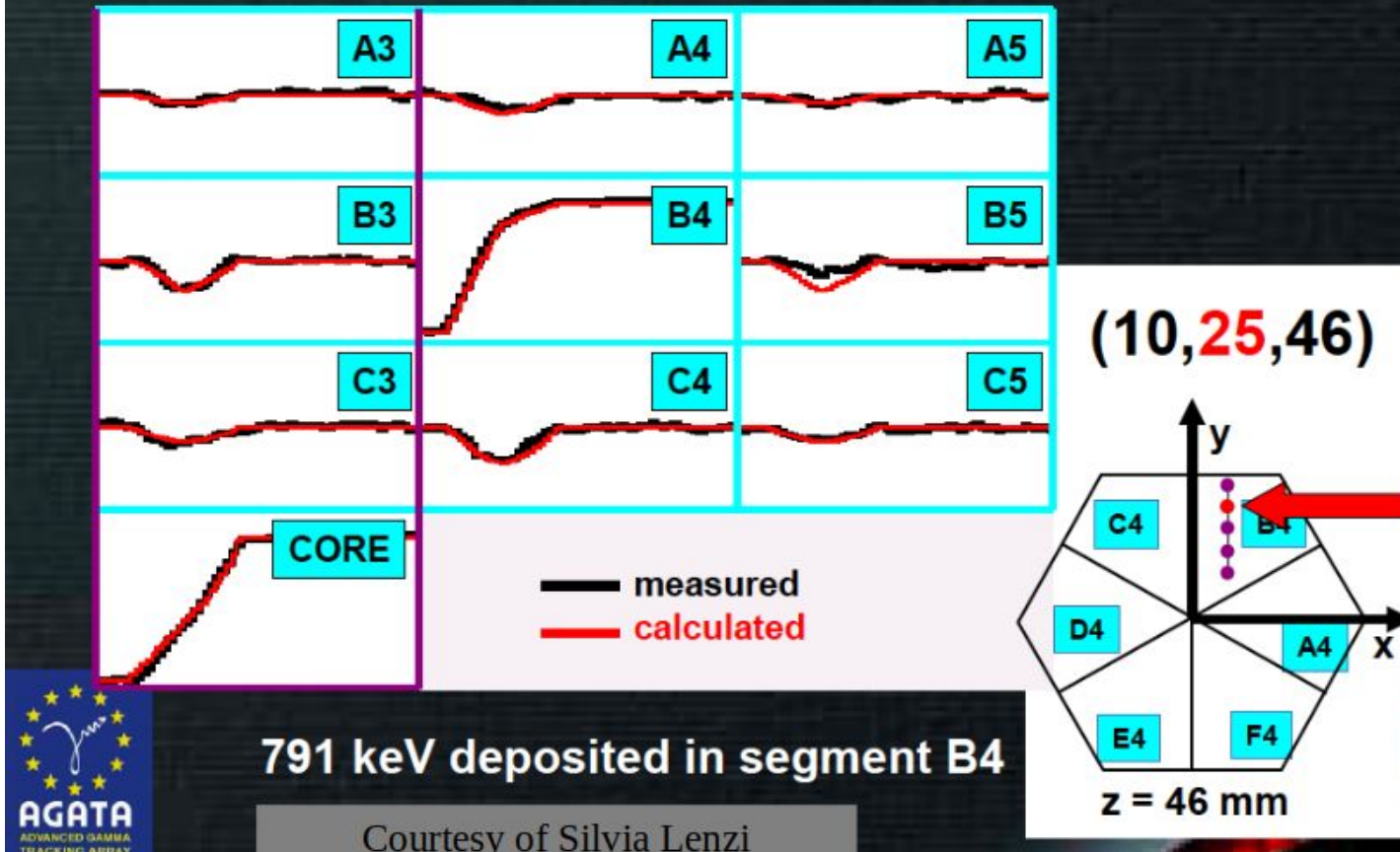
The pulse-shape analysis process



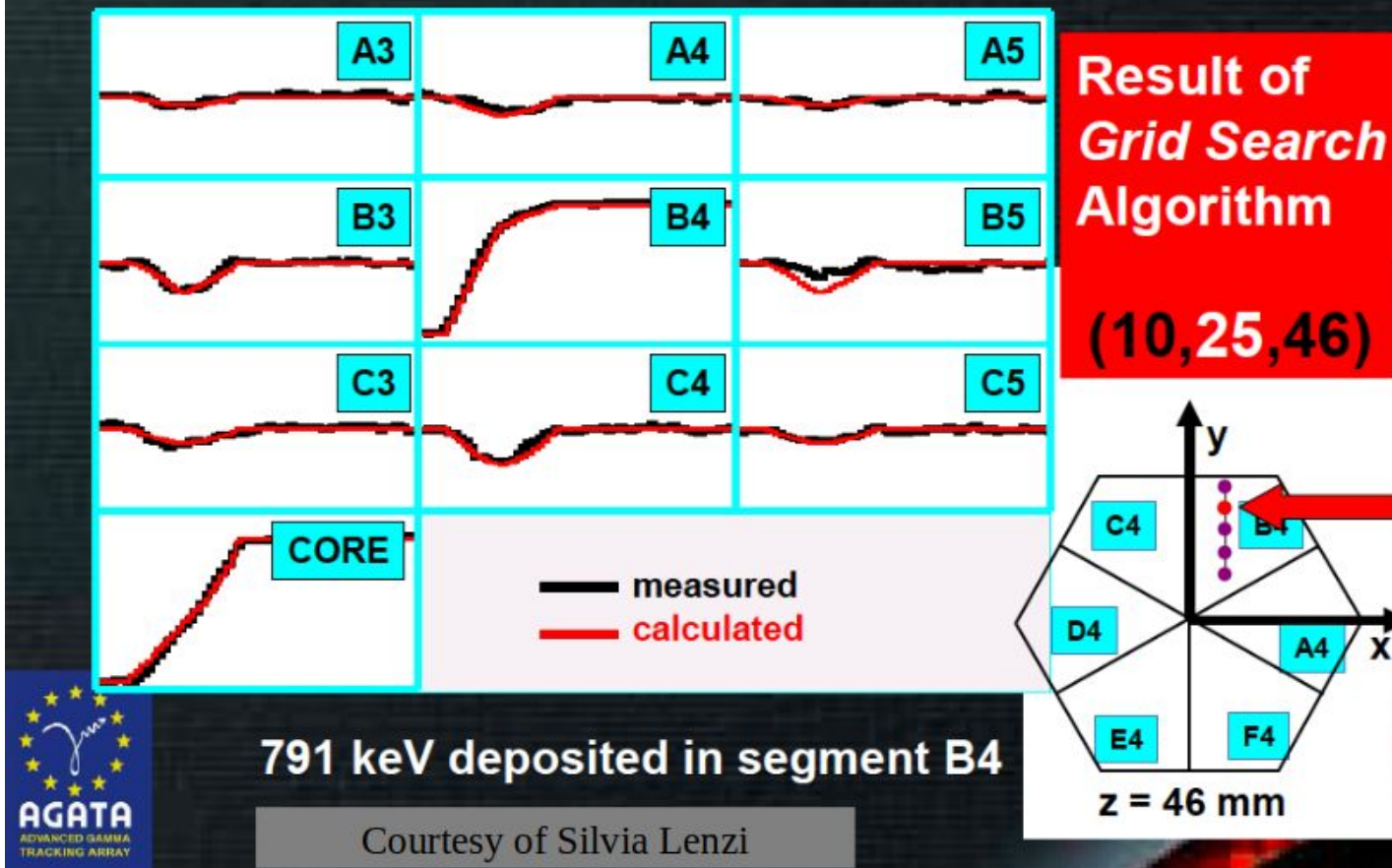
The pulse-shape analysis process



The pulse-shape analysis process

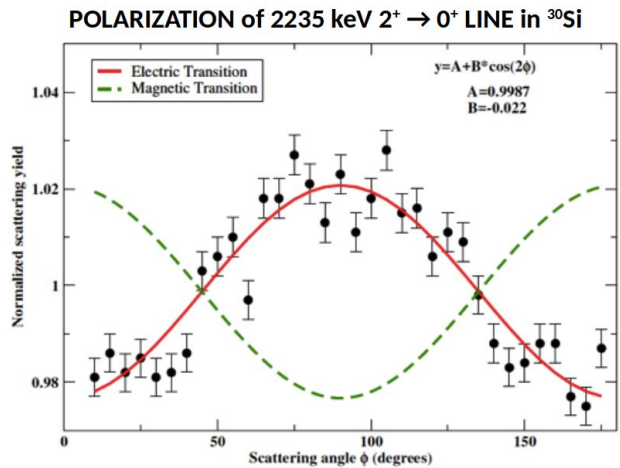
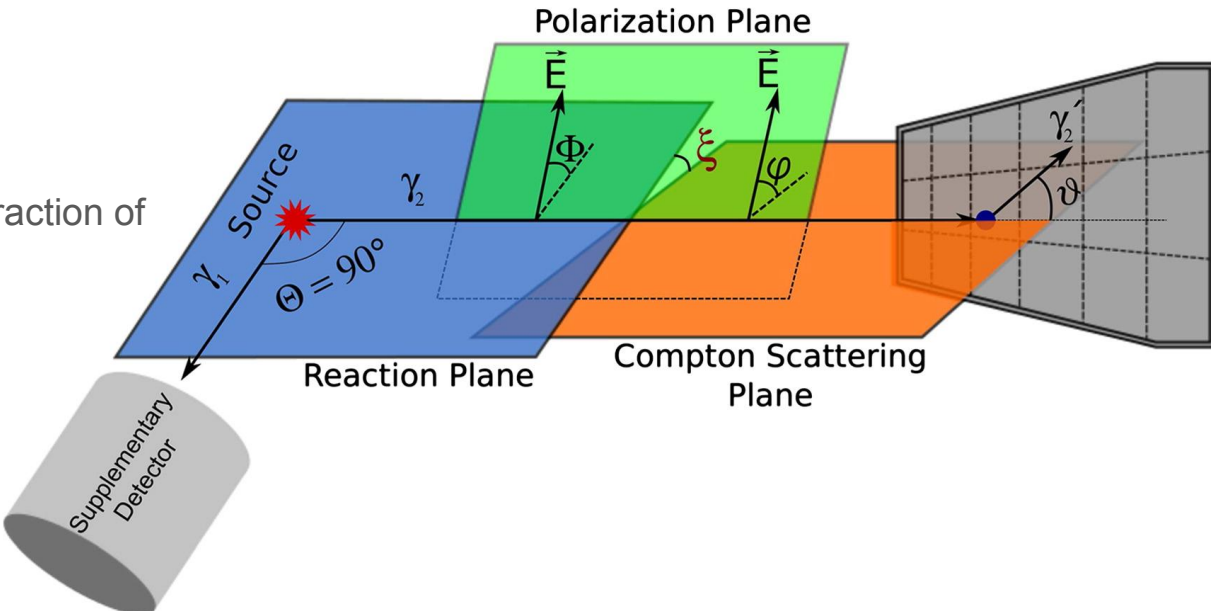


The pulse-shape analysis process



Polarization

- Requires first and second interaction of Compton scattered photon



$$\frac{d\sigma}{d\Omega}(\theta, \phi) = \frac{r_0}{2} \left(\frac{E'_\gamma}{E_\gamma} \right)^2 \left[\frac{E_\gamma}{E'_\gamma} + \frac{E'_\gamma}{E_\gamma} - 2 \sin^2 \theta \cos^2 \phi \right]$$

Recaps

- Important for Nuclear in-beam experiments:
 - Energy resolution: Doppler correction, requiring knowledge of location of first interaction
 - Peak-to-total: Tracking enables to reconstruct full energy of initial photon
 - Efficiency: Large 4PI arrays
- As a bonus: Polarization of photon can be measured
- But: Event reconstruction extremely complex and computational demanding

GRETINA/GRETA and AGATA

- P. Fallon, et. al, GRETINA and Its Early Science, Annual Review of Nuclear and Particle Science,66, 1, 321-339 (2016)
- S. Paschalidis, et. al., The performance of the Gamma-Ray Energy Tracking In-beam Nuclear Array GRETINA, Nuclear Instruments and Methods in Physics Research Section A, 709 44-55, (2013)
- GRETA Whitepaper: http://fribusers.org/documents/2014/GRETA_whitepaper.pdf
- AGATA detectors: <https://conferences.lbl.gov/event/121/session/7/contribution/7>

2017 International Germanium Detector Technology Workshop:

- <https://conferences.lbl.gov/event/121/>

PHD Thesis

- <https://www.mpi-hd.mpg.de/gerda/public/2015/phd2015-MarcoSalathe.pdf>